Low-Frequency Noise in Charge-Density-Wave Quantum Materials

Alexander A. Balandin
Department of Electrical and Computer Engineering
Materials Science and Engineering Program
University of California, Riverside, USA

The Ettore Majorana School, Erice, Sicily, Italy

April 2022

UNIVERSITY OF CALIFORNIA
UC RIVERSIDE

| Nano-Device Laboratory >

City of Riverside

UCR Botanic Gardens

UCR Bell Tower

Joshua Tree Park

UCR Engineering Building

Outline

- → Part I: Noise Background and History
- → Part II: Noise in Graphene
  - → Noise reduction and other highlights
  - → Graphene under irradiation
- → Part III: Noise as the Signal
  - → Graphene *vs.* MoS_2
- → Part IV: Noise in 2D CDW Materials
  - → 2D CDW quantum materials
  - → Noise spectroscopy of CDWs
- → Part V: 1D van der Waals Materials
  - → Going from 2D to 1D – again!

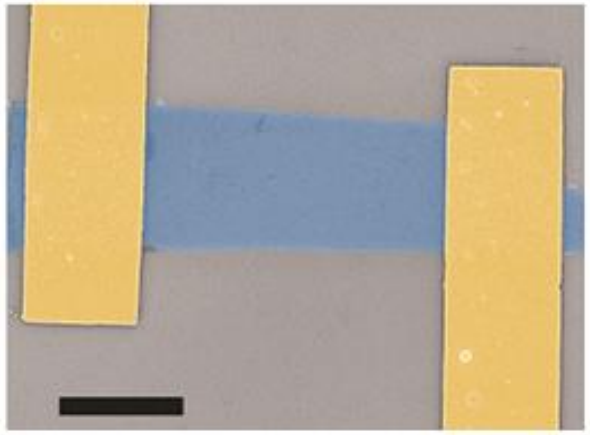

Nano-Device Laboratory

Part IV: Charge Density Waves

Normal state $T > T_c$

Electron Density $\rho_e = const$

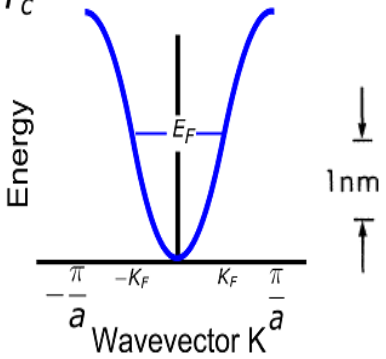

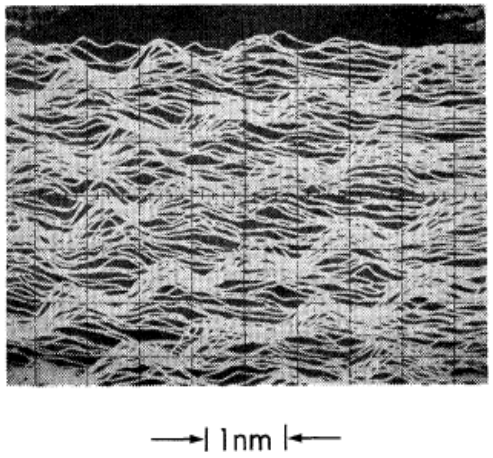

R.V. Coleman, *Phys. Rev. Lett.*, **55**, 394 (1985).

Peierls state $T < T_c$

Electron Density $\rho_e = \rho_0 + \rho_1 cos(qx + \lambda_c)$

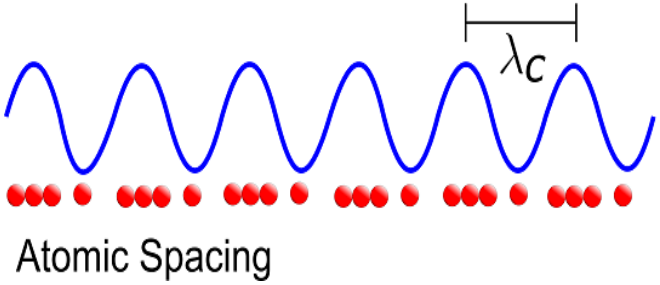

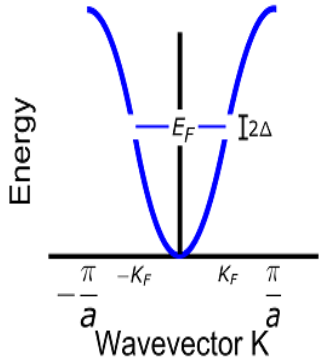

$\lambda=2\pi/k_F$ in general is not commensurate with the lattice

Macroscopic quantum phenomena: coherence length >1 μm

Depinning and Sliding of CDWs in Bulk Quasi-1D CDW Materials

CDWs in metallic crystals form due to the wave nature of electrons – a manifestation of quantum mechanical wave nature of electrons – causing the electronic charge density to become spatially modulated.

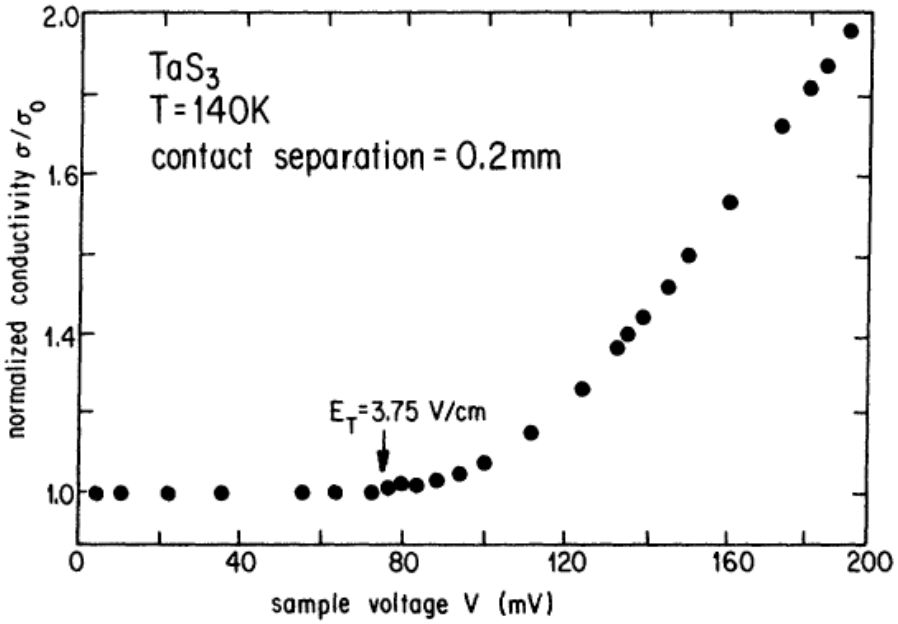

G. Gruner, et al., Phys. Rev. B, 23, 6813 (1981).

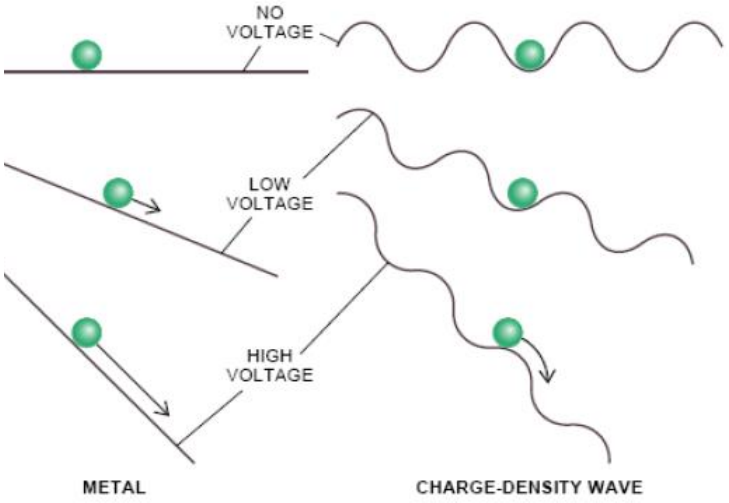

For fields larger than a threshold field E_T, the sliding CDW provides a second conduction path next to a single-particle electron conduction. Macroscopically this leads to non-linear electrical conductivity and oscillations for large fields.

"Narrow Band Noise" in Bulk Quasi-1D CDW Materials

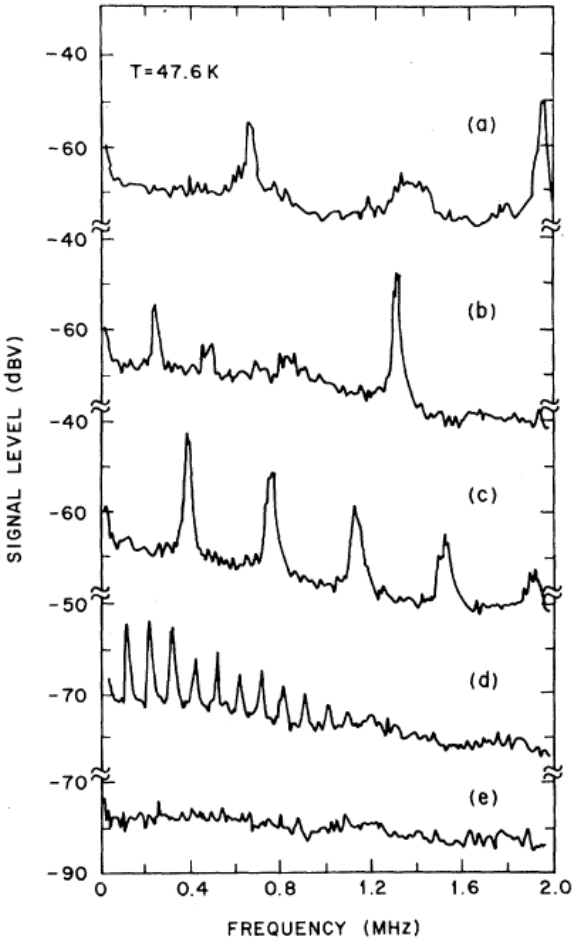

Sliding-Mode Conductivity in $NbSe_3$: Observation of a Threshold Electric Field and Conduction Noise

R. M. Fleming and C. C. Grimes
Bell Laboratories, Murray Hill, New Jersey 07974
(Received 15 March 1979)

FIG. 3. Output of on-line spectrum analyzer for selected values of current. Increasing current from zero (e) to a value above threshold (d) results in an increase of broad-band noise plus a discrete frequency with numerous harmonics. The frequency increases with current and at higher currents (b) a second frequency appears. Currents and dc voltages (a) $I = 270\ \mu A$, $V = 5.81$ mV, (b) $I = 219\ \mu A$, $V = 5.05$ mV, (c) $I = 154\ \mu A$, $V = 4.07$ mV, (d) $I = 123\ \mu A$, $V = 3.40$ mV, (e) $I = V = 0$. Sample cross section $\approx 136\ \mu m^2$.

- "Narrow band noise" (NBN) is a direct evidence of CDW de-pinning and sliding.
- Not noise but AC component in current

Current Oscillations in Bulk Quasi-1D CDW Materials

Narrow band noise (NBN)

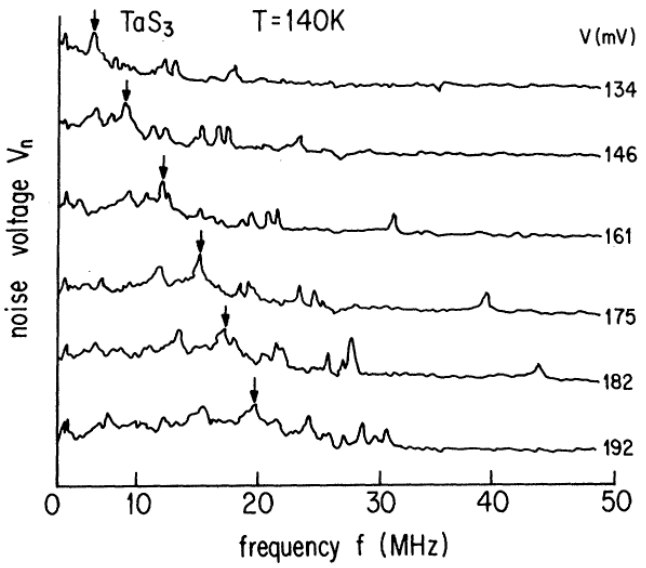

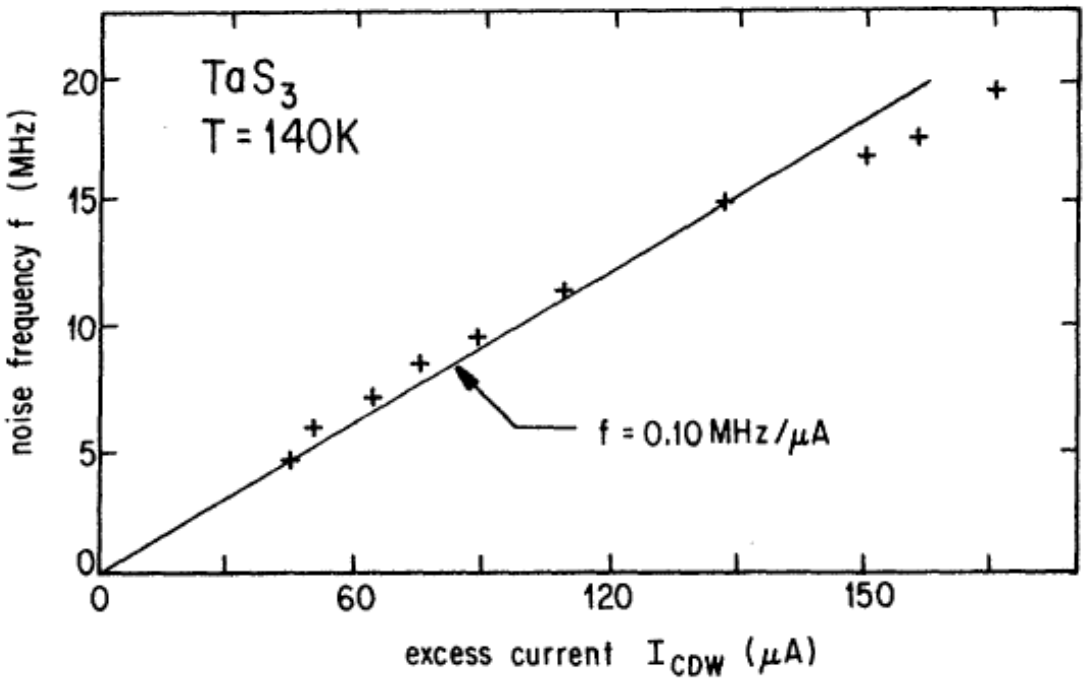

G. Gruner, et al., Phys. Rev. B, 23, 6813 (1981).

→ Excess current, $I_{CDW}=I-I_N$, attributed to the CDW sliding

→ Fundamental frequency $f=(1/ne\Lambda A)\times I_{CDW}$

Renewal of Interest to CDW Materials: Quasi-2D Films of TMD

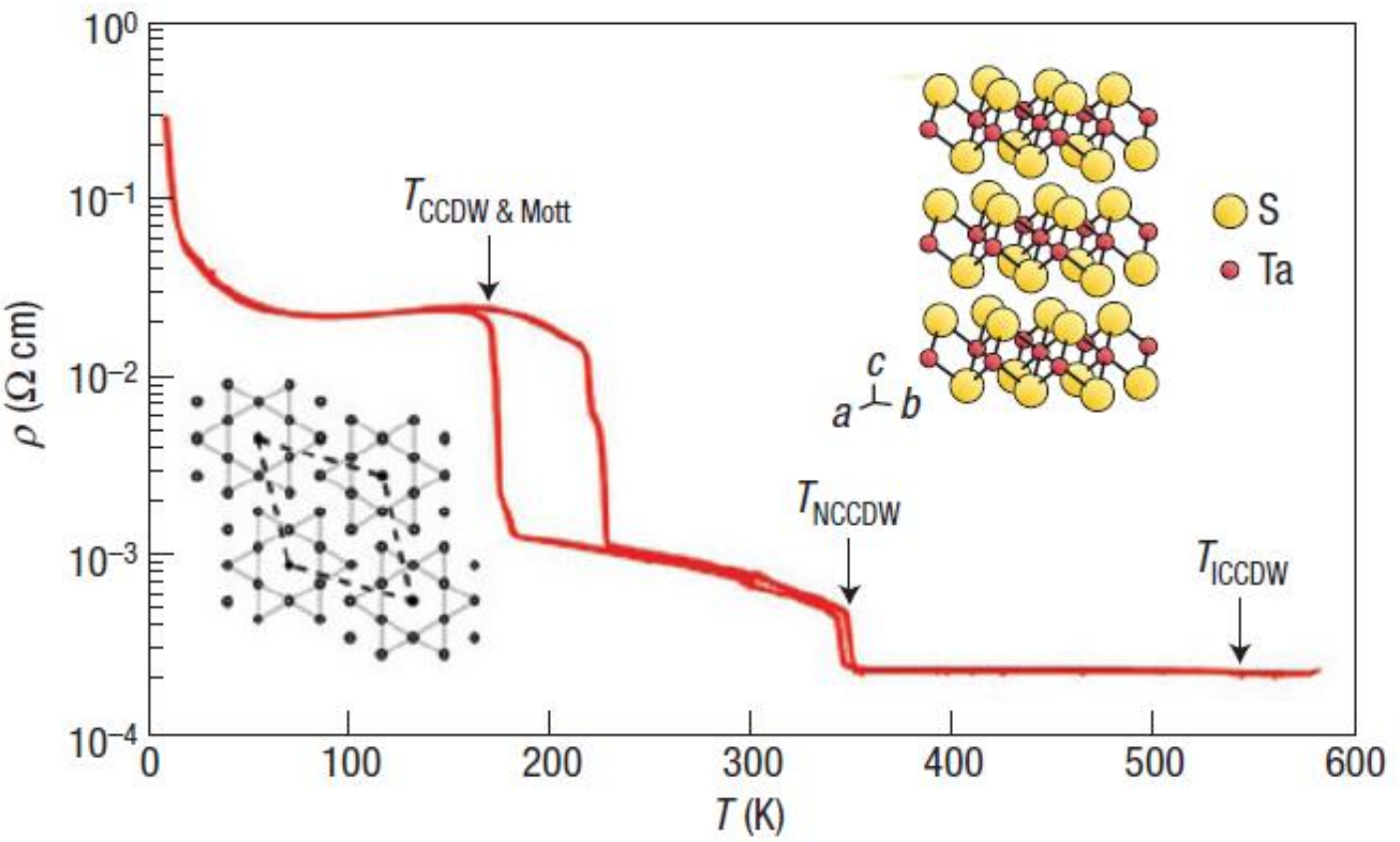

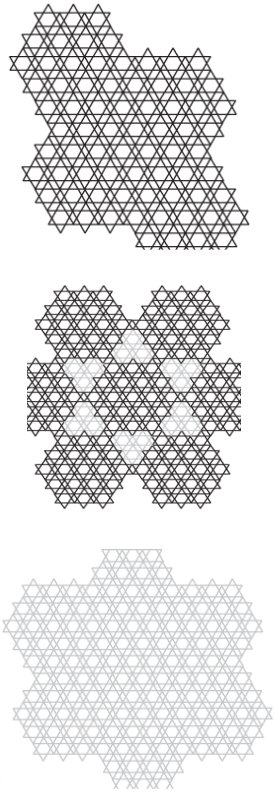

B. Sipos, A.F. Kusmartseva, A. Akrap, H. Berger, L. Forró, and E. Tutiš, Nature Mater., 7, 960 (2008).

Illustration of the Structure of 1T-TaS_2 at Various Temperatures

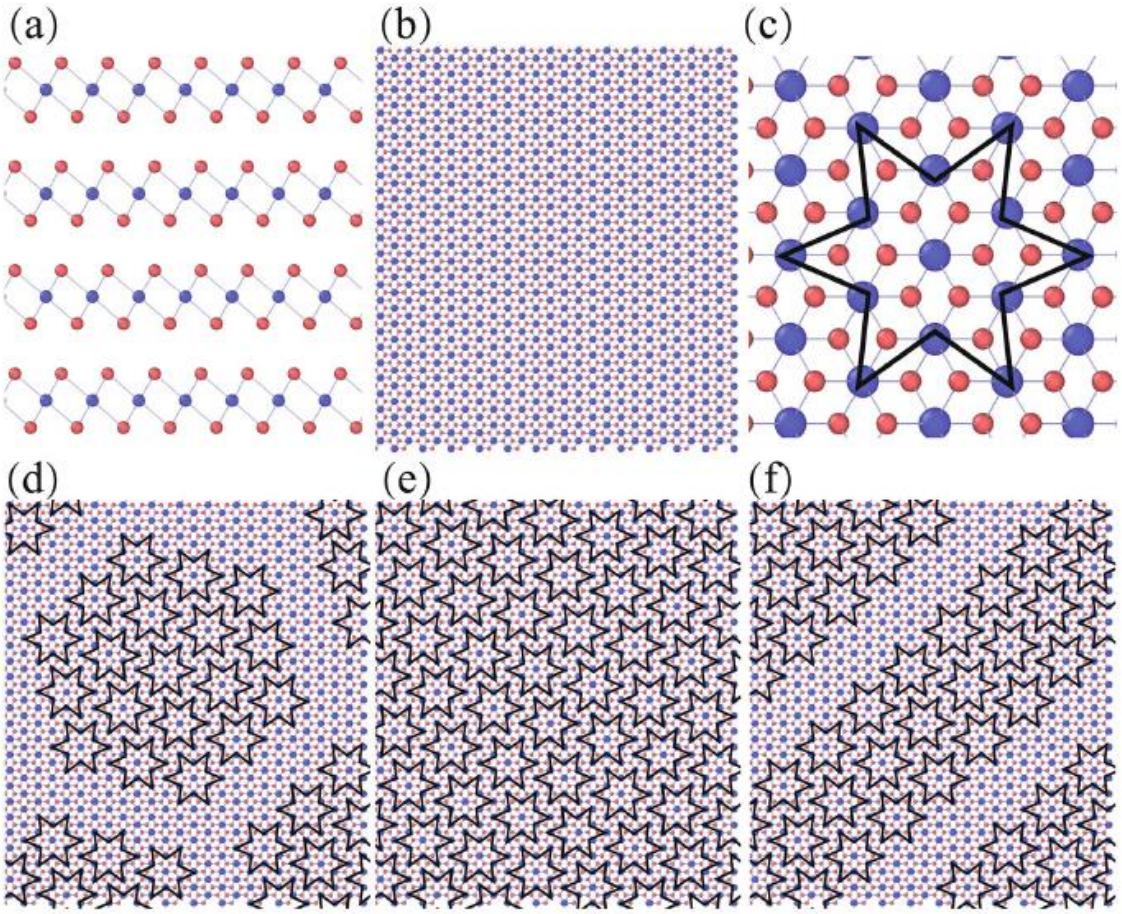

Figure 1. Illustration of the structure of 1T-TaS_2 at various temperature. (a) Side view of 1T-TaS_2. (b) Top view of 1T-TaS_2. (c) 'Star of David' where 12 Ta atoms within the layer move to the 13th central Ta atom. (d) NC-CDW phase in which 'star of David' clusters formed several separate hexagonal array structures (e) C-CDW phase, which consists of a uniform distribution of 'stars of David'.

W. Wang, D. Dietzel and A. Schirmeisen, Scientific Reports, (9, 7066 (2019)

Dimensionality Effects on CDW Transitions in Quasi-2D Films of TMDs

1T-$TaSe_2$

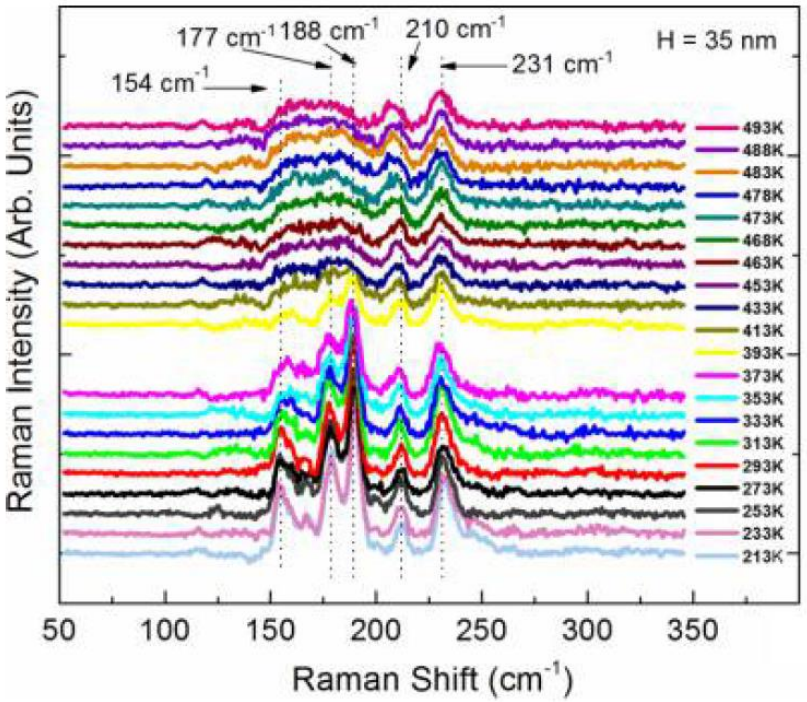

R. Samnakay, D. Wickramaratne, T. R. Pope, R. K. Lake, T. T. Salguero, and A. A. Balandin, Nano Lett., 15, 2965 (2015).

1T-TaS_2

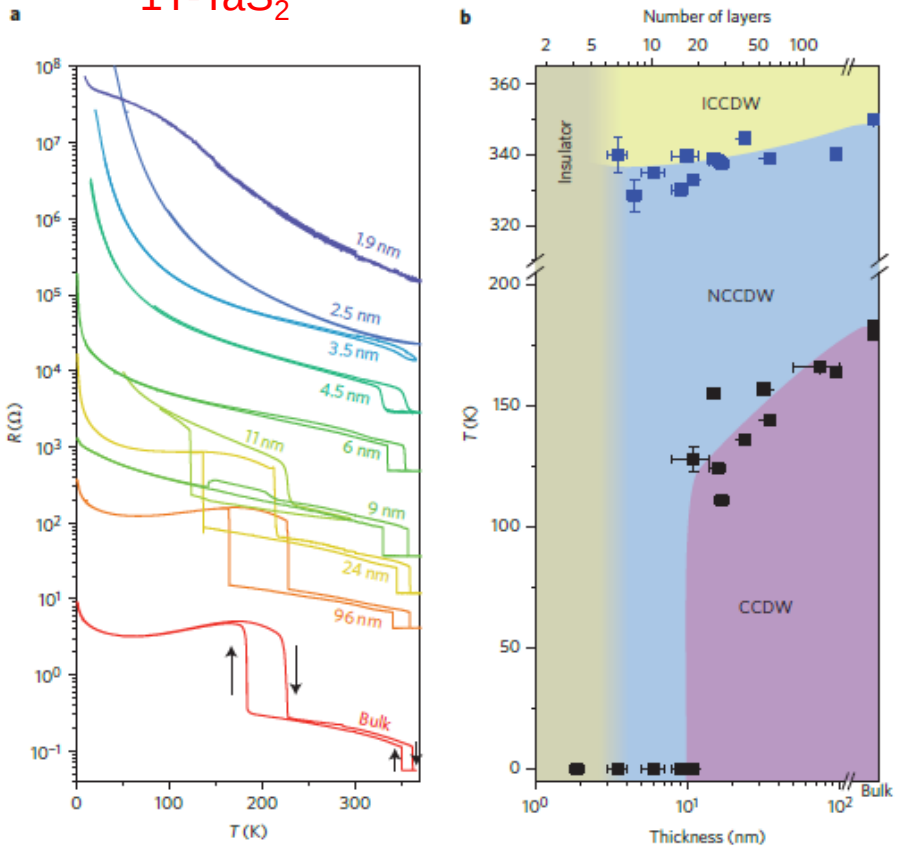

Y. Yu et al, Nature Nano, 10, 270 (2015)

Types of CDW Phase Transitions

- There is no uniform mechanism to explain the origin of CDW in different systems, which means truly quantitative predictions of CDW properties for a new material are practically impossible.
- Type I – CDW in 1D Peierls' model: band-gap (or FSN) in electronic structure, Kohn anomaly in phonon spectra, a structural transition in lattice and a metal–insulator transition. Examples: NbS_3; TaS_3
- Type II – CDW in 2D electron–phonon coupling model: The CDW in 2D is not driven by FSN. Instead, the CDW phases are dictated by the q-dependent electron–phonon coupling (EPC). Examples: $NbSe_2$; $TaSe_2$; TaS_2
- Type III – CDW with 3D character: charge modulation or charge ordering with no indication of FSN or EPC as the driving force. Examples: rare earth systems such as $R_5Ir_4Si_{10}$

X. Zhu, J. Guo, J. Zhang and E. W. Plummer (2017) Misconceptions associated with the origin of charge density waves, Advances in Physics: X, 2:3, 622-640, DOI: 10.1080/23746149.2017.1343098

Device Structure and Contacts

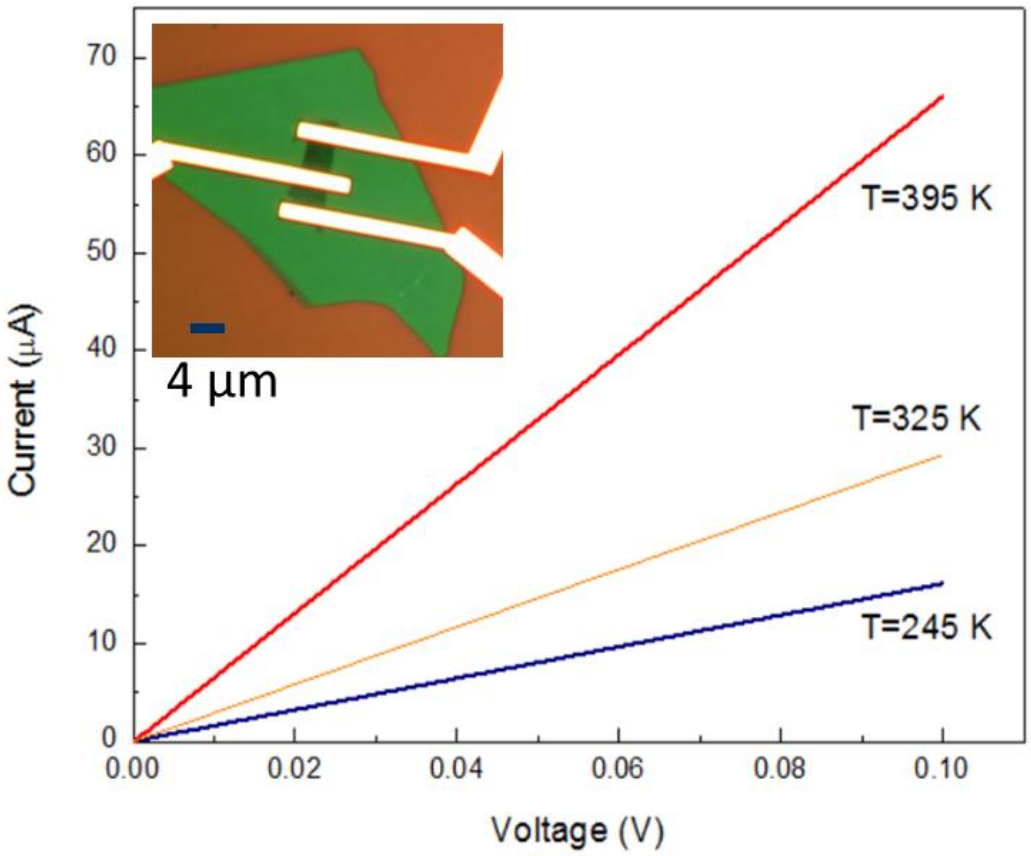

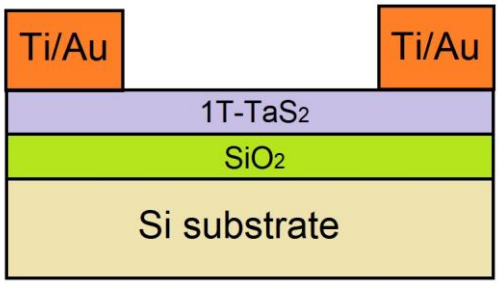

Channel thickness:
t = 6 nm - 9 nm

Contacts:
Pd/Au (15 nm / 60 nm)

→ The h-BN cap provides air stable passivation for the 1T-TaS_2.

→ The edge contacts provide good Ohmic contacts to the 1T-TaS_2.

Low-Voltage I-V Characteristics of Thin Film 1T-TaS_2

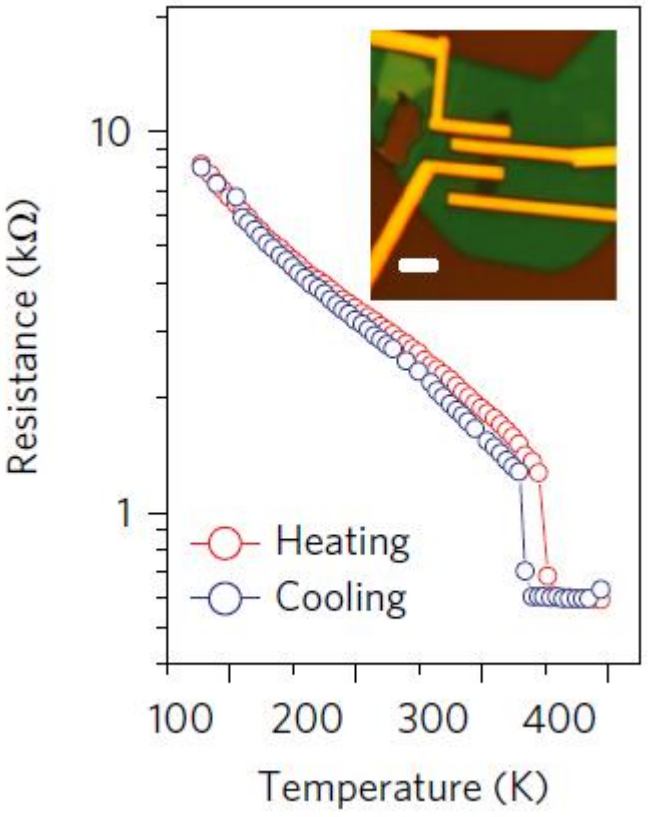

→ Temperature-dependent resistance measurements for 1T-TaS_2. The NC-CDW–IC-CDW and IC-CDW–NC-CDW transitions happen at 350 K and 340 K during the heating and cooling process, respectively. The resistance is measured at low voltage (V=20 mV).

→ Resistances match

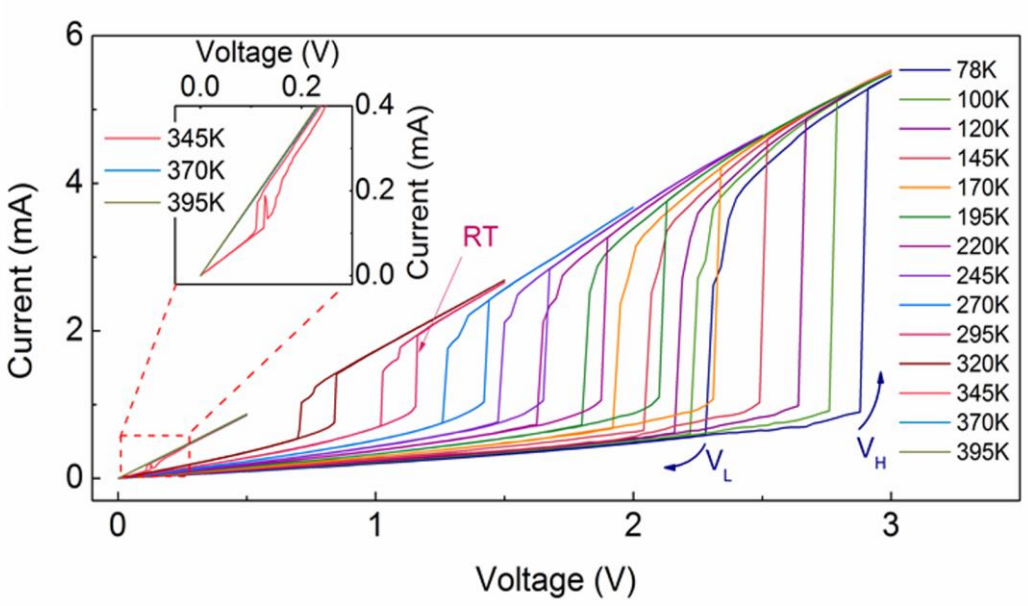

G. Liu, B. Debnath, T. R. Pope, T. T. Salguero, R. K. Lake, and A. A. Balandin, Nature Nano, 11, 845 (2016).

Two-Terminal CDW Quasi-2D 1T-TaS_2 Devices

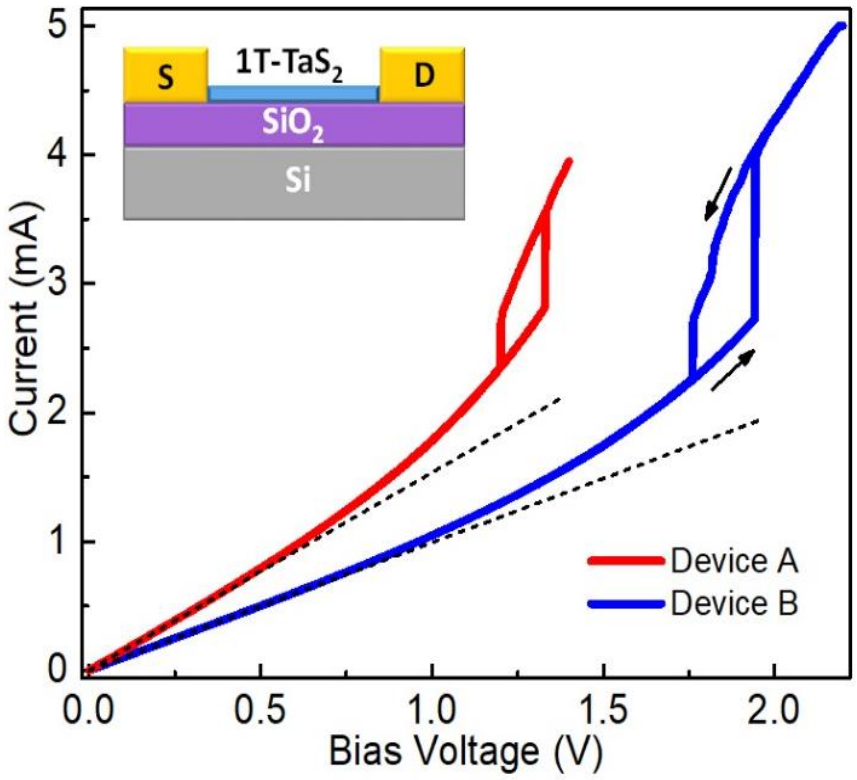

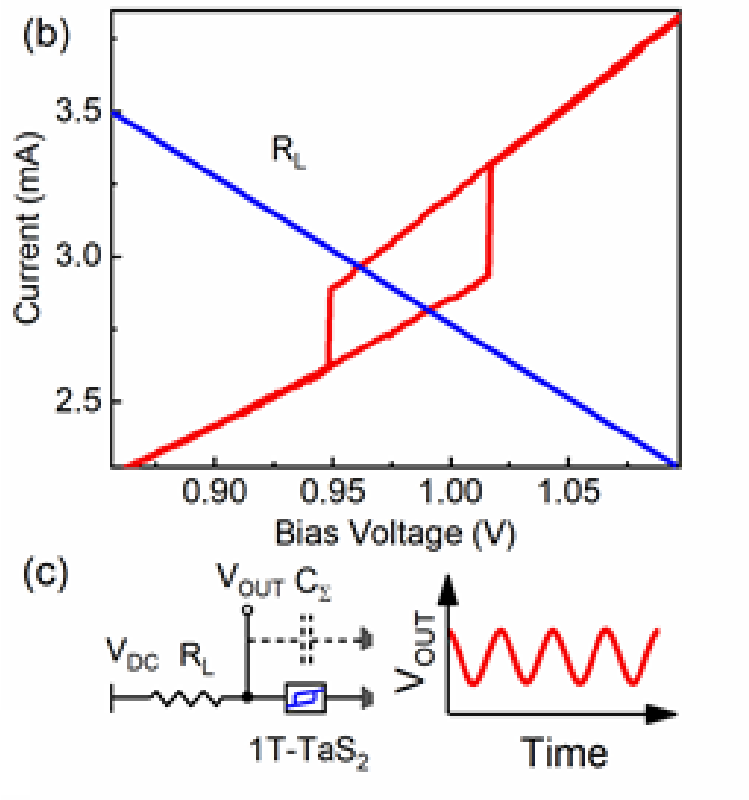

→ Negative feedback

Room-Temperature CDW "Quantum" Device

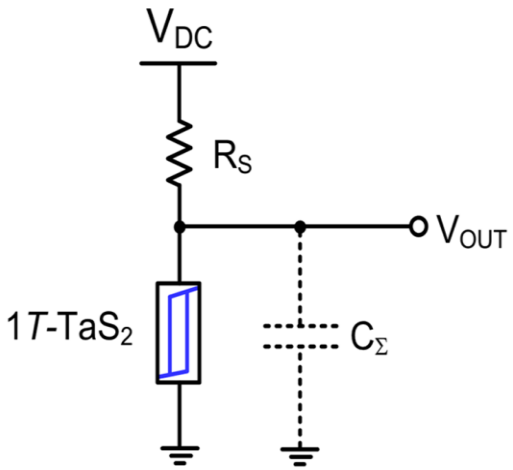

Different operation mechanism from early devices – no de-pinning

Allows for high T operation

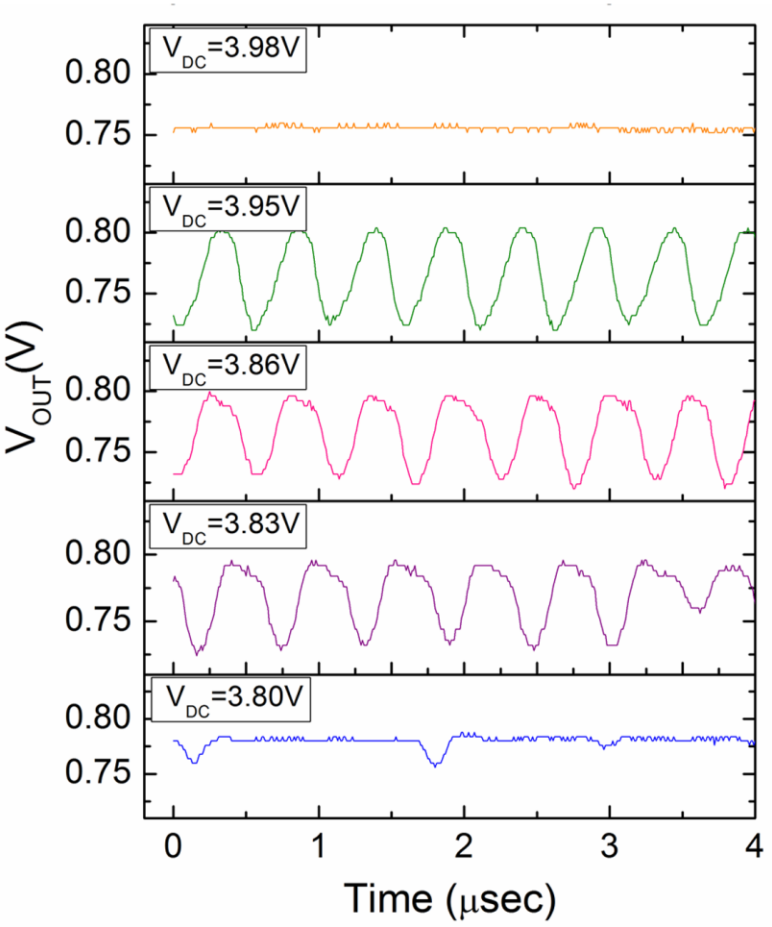

→Circuit schematic of the oscillator consists of the 1T-TaS_2 film, a series connected load resistor, and a lumped capacitance from the output node to ground. The load resistance is 1 kΩ.

→Voltage oscillations under different V_{DC}. The circuit oscillates when V_{DC} is within the range of 3.83-3.95 V. The frequency is 1.77 MHz, 1.85 MHz, and 2 MHz when V_{DC} is 3.83, 3.86 and 3.95 V, respectively.

Integrated 1T-TaS_2 – h-BN – Graphene VCO

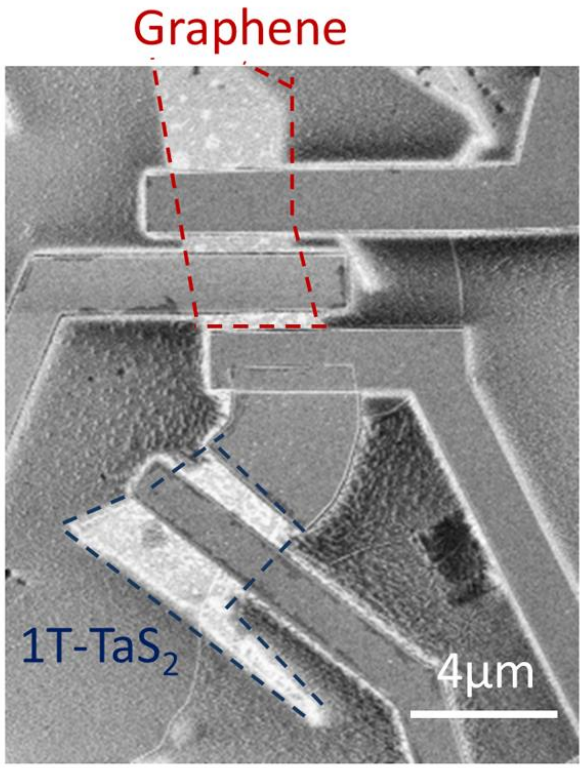

The SEM image of the integrated 1T-TaS_2–BN–graphene voltage controlled oscillator. The graphene and the TaS_2 are highlighted by dashed lines.

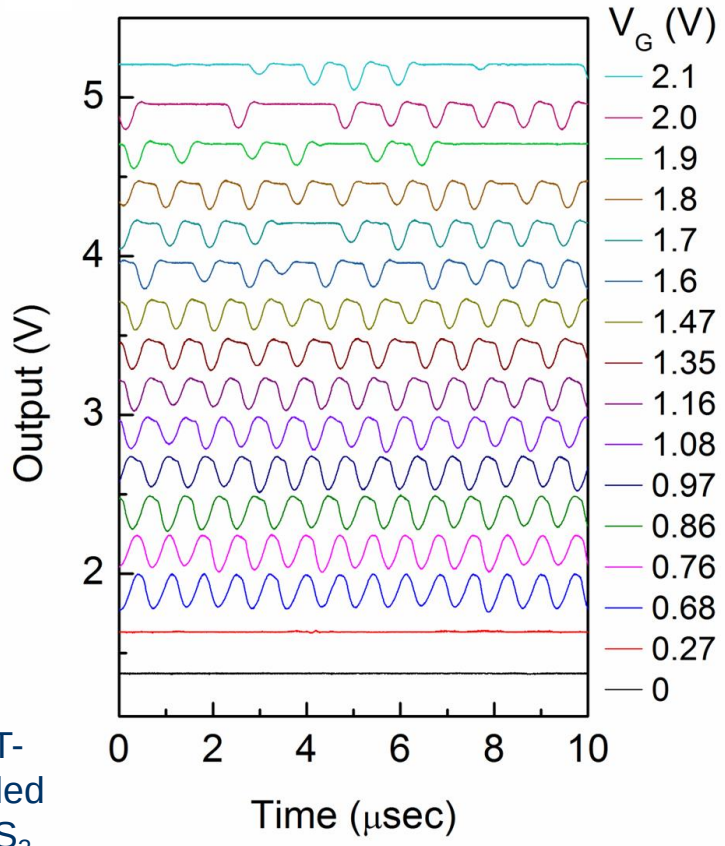

Output waveforms at different gate biases when V_{DC} is fixed at 3.65 V. The oscillation frequency is tunable with gate biases in the range of 0.68 V to 1.8 V. The different waveforms are vertically offset of 0.25 V for clarity.

G. Liu, B. Debnath, T. T. Salguero, R. K. Lake, and A. A. Balandin, Nature Nano, 11, 845 (2016).

1T-TaS_2 – h-BN – Graphene CDW VCO

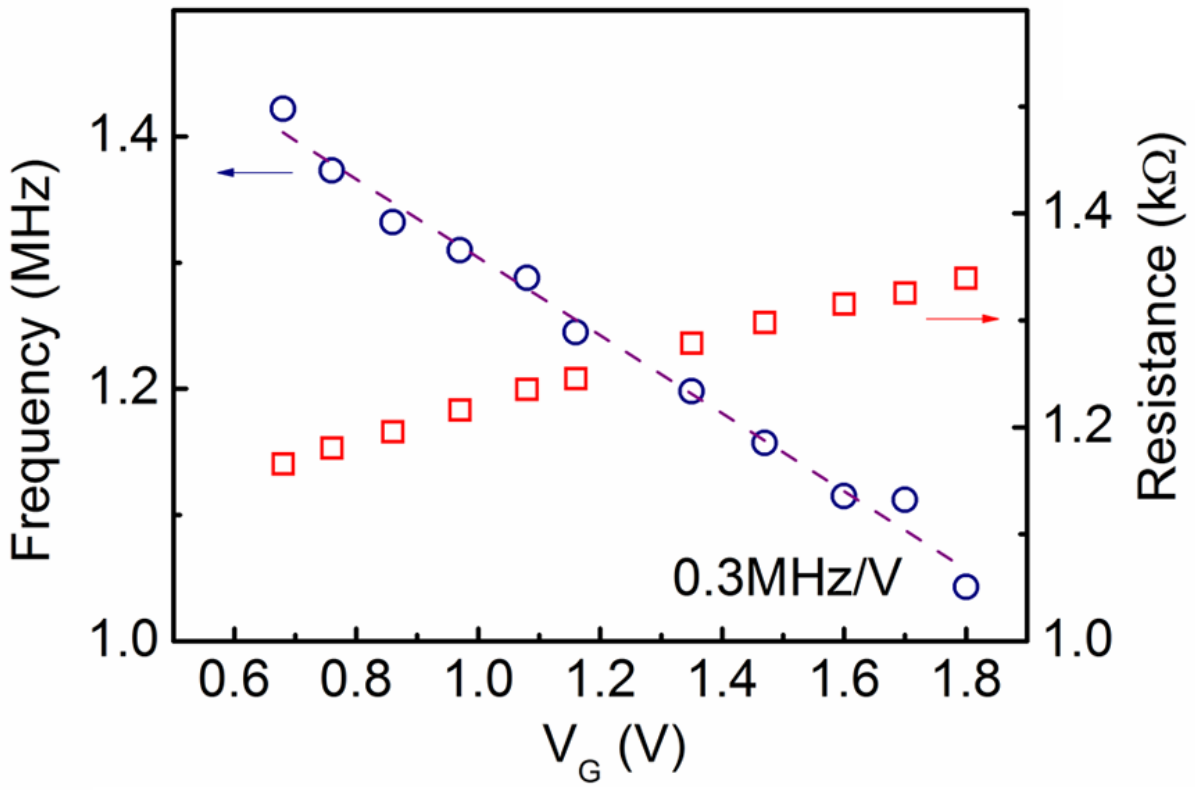

The dependence of oscillation frequency as function of gate bias.

Blue circles show the frequency of the oscillation under increased gate bias. The frequency can be adjusted monotonically with the tuning sensitivity of 0.3M Hz/V.

The red squares are the resistance value of the G-FET under different gate biases with fixed V_{DC}=2.4V.

G. Liu, B. Debnath, T. R. Pope, T. T. Salguero, R. K. Lake, and A. A. Balandin, Nature Nano, 11, 845 (2016).

1T-TaS_2 CDW Devices Under X-Ray Irradiation

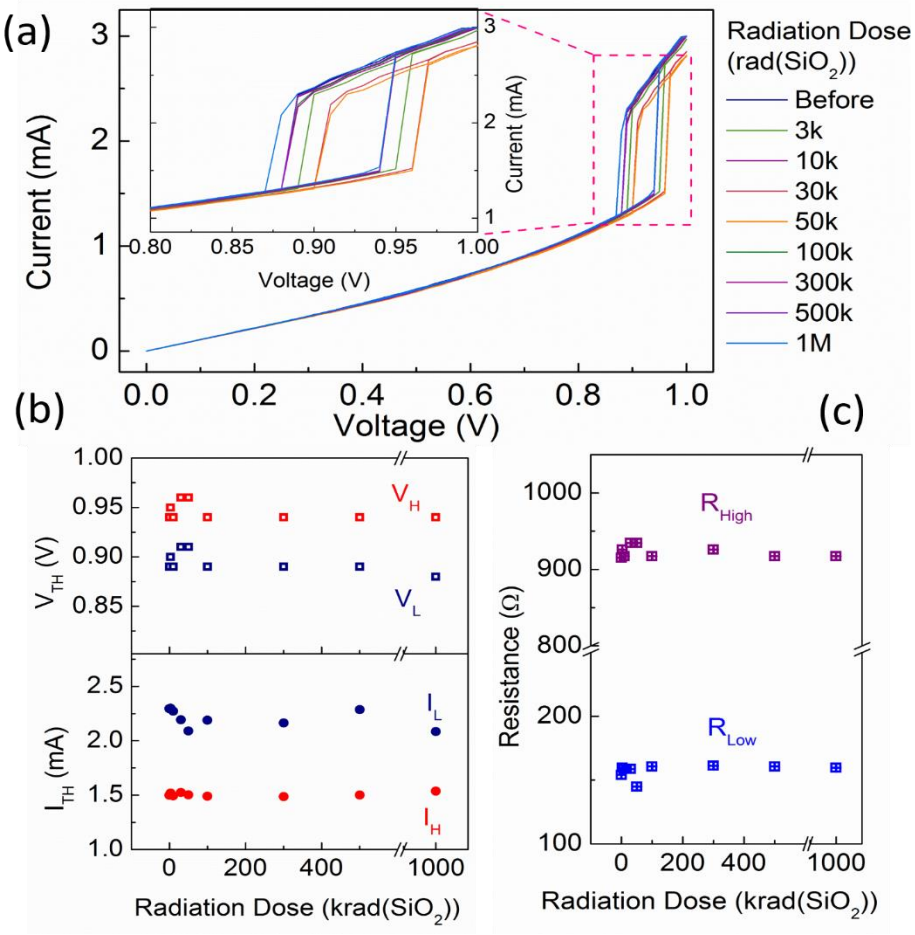

TID response of 1T-TaS_2 devices up to 1 M rad (SiO_2). (a) I-V curves measured after each X-ray irradiation step. (b) Threshold voltages, V_H and V_L, threshold currents, I_H and I_L as function of dose. (c) Extracted resistance at the high resistance and low resistance states as a function of dose.

Carrier concentration:
10^{21} cm^{-2} - 10^{22} cm^{-2}

G. Liu, E. X. Zhang, C. Liang, M. Bloodgood, T. Salguero, D. Fleetwood, A. A. Balandin, "Total-ionizing-dose effects on threshold switching in 1T-TaS_2 charge density wave devices," IEEE Electron Device Letters, 38, 1724 (2017).

Radiation Hardness of CDW Devices

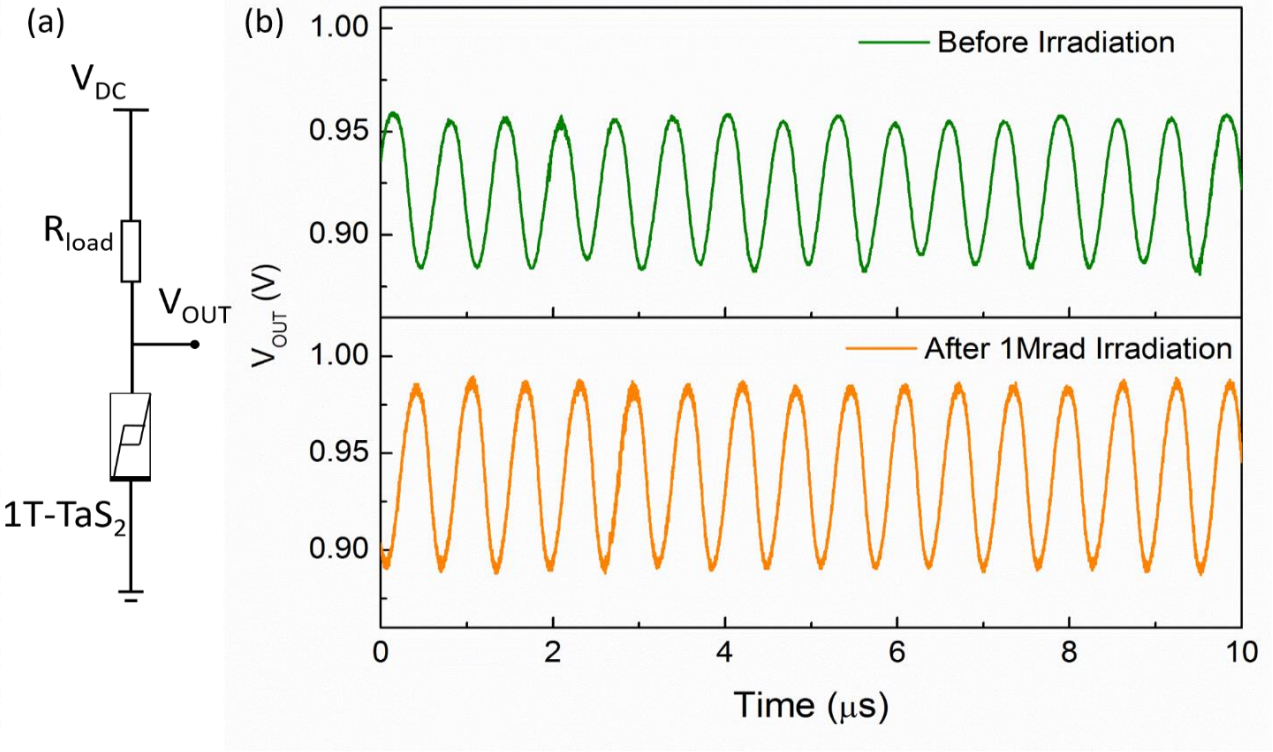

(a) Circuit schematic diagram of a self-sustaining oscillator implemented with one 1T-TaS_2 device and a load resistor.

(a) Oscillation waveform before and after 1 Mrad(SiO_2) X-ray irradiation

G. Liu, E. X. Zhang, C. Liang, M. Bloodgood, T. Salguero, D. Fleetwood, A. A. Balandin, "Total-ionizing-dose effects on threshold switching in 1T-TaS_2 charge density wave devices," IEEE Electron Device Letters, 38, 1724 (2017).

Using Noise Spectroscopy to Assess Radiation Damage - Proton Bombardment

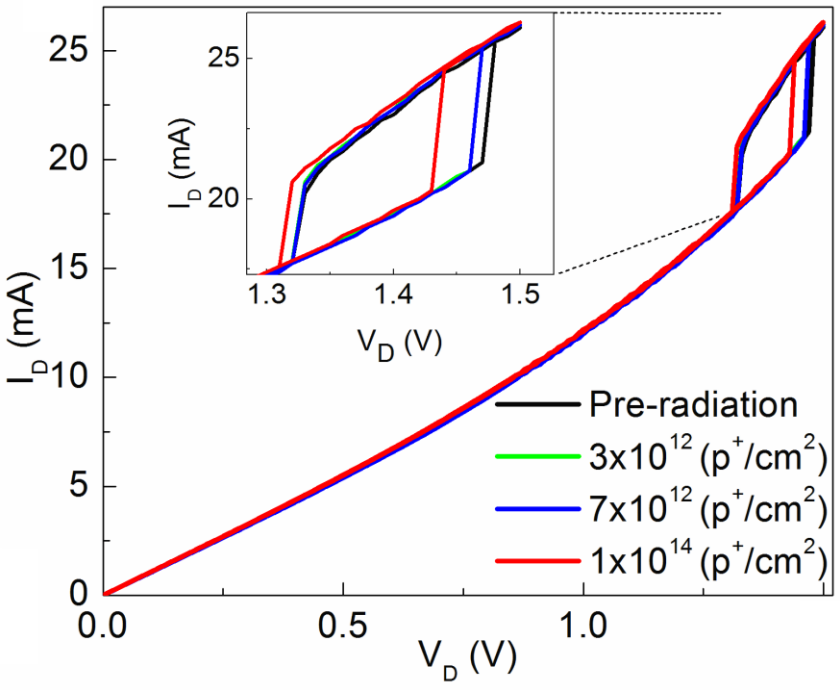

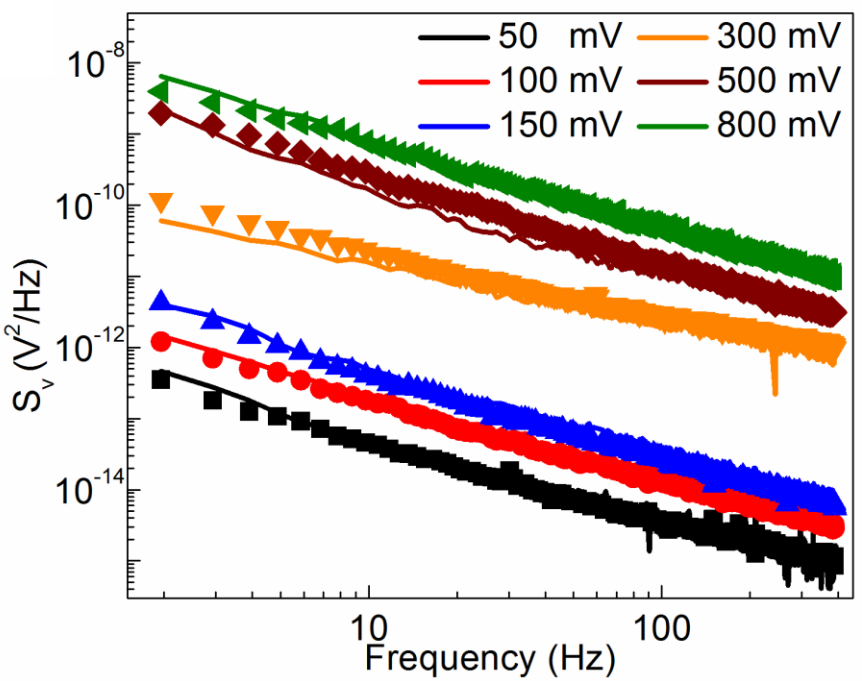

The quasi-two-dimensional (2D) 1T-TaS_2 channels show a *remarkable* immunity to bombardment with the high-energy 1.8 MeV protons to, at least, the irradiation fluence of 10^{14} H^+cm^{-2}.

A. K. Geremew, F. Kargar, E. X. Zhang, S. E. Zhao, E. Aytan, M. A. Bloodgood, T. T. Salguero, S. Rumyantsev, A. Fedoseyev, D. M. Fleetwood and A. A. Balandin, Nanoscale, 11, 8380 (2019).

Monitoring CDW Phase Transitions with Noise Spectroscopy

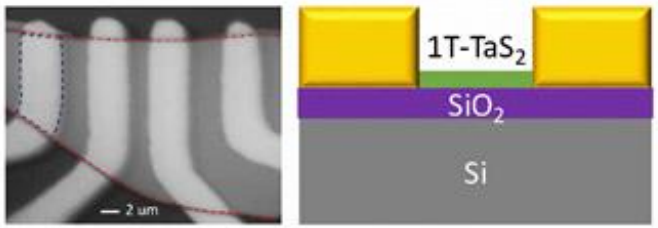

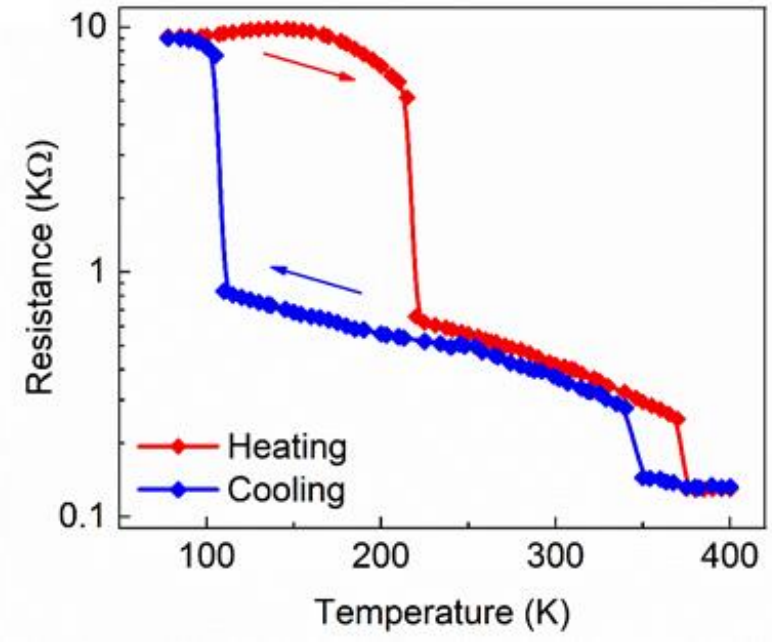

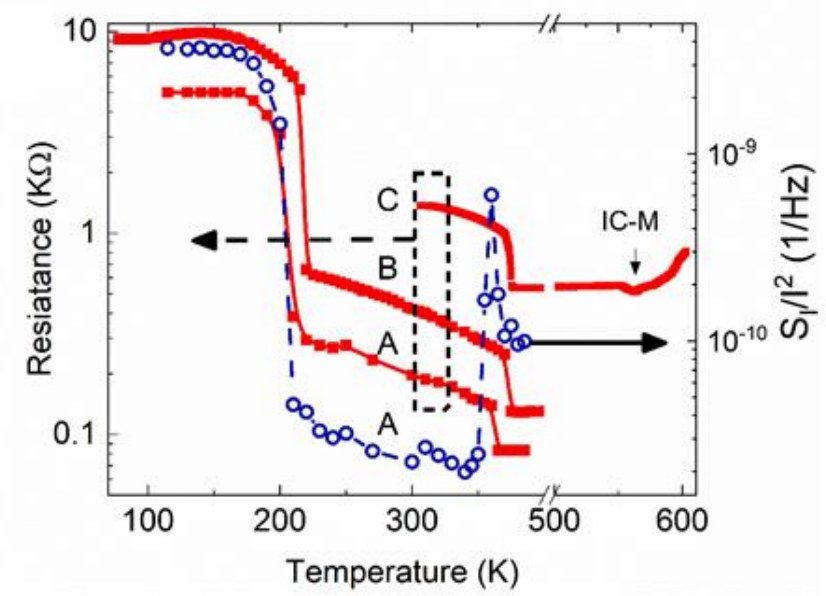

→Optical image of a representative device (left panel) and a schematic of the device layered structure (right panel). The scale bar is 2 μm.

→Resistance as function of temperature for cooling (blue curve) and heating (red curve) cycles conducted at the rate of 2 K per minute.

Noise Spectroscopy of CDW Transitions

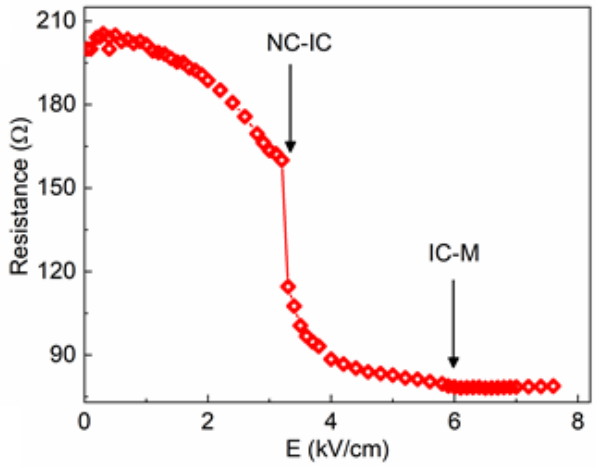

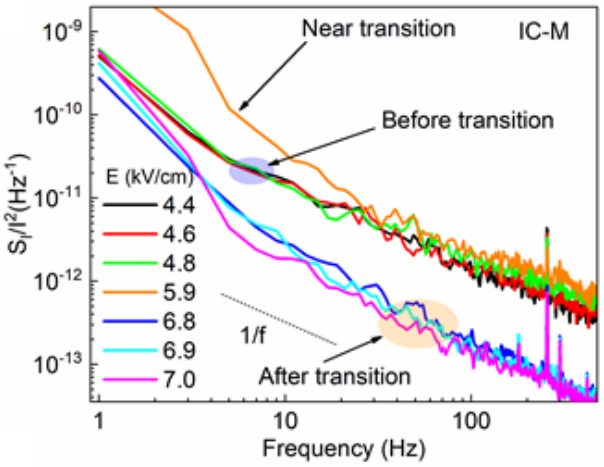

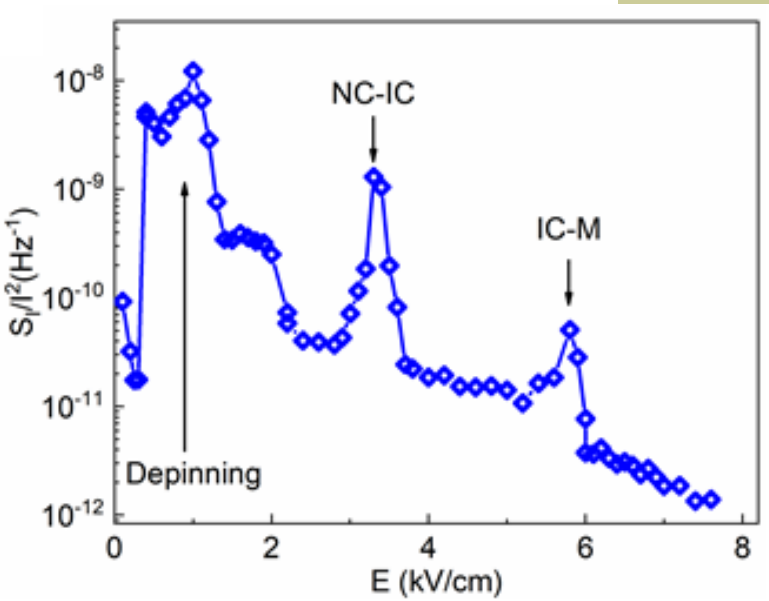

→ Resistance as a function of the applied electric field measured at RT.
→ Noise spectral density as the function of frequency for several values of the electric field, which include the point of transition from the IC-CDW to the normal metallic phase.
→ Noise spectral density, measured at f=10 Hz, as the function of the electric field.

A. K. Geremew, S. Rumyantsev, F. Kargar, B. Debnath, A. Nosek, M. A. Bloodgood, M. Bockrath, T. T. Salguero, R. K. Lake, and A. A. Balandin, ACS Nano, 13, 7231 (2019).

Can the CDW Switching be Fast Even If It is Induced by Heating?

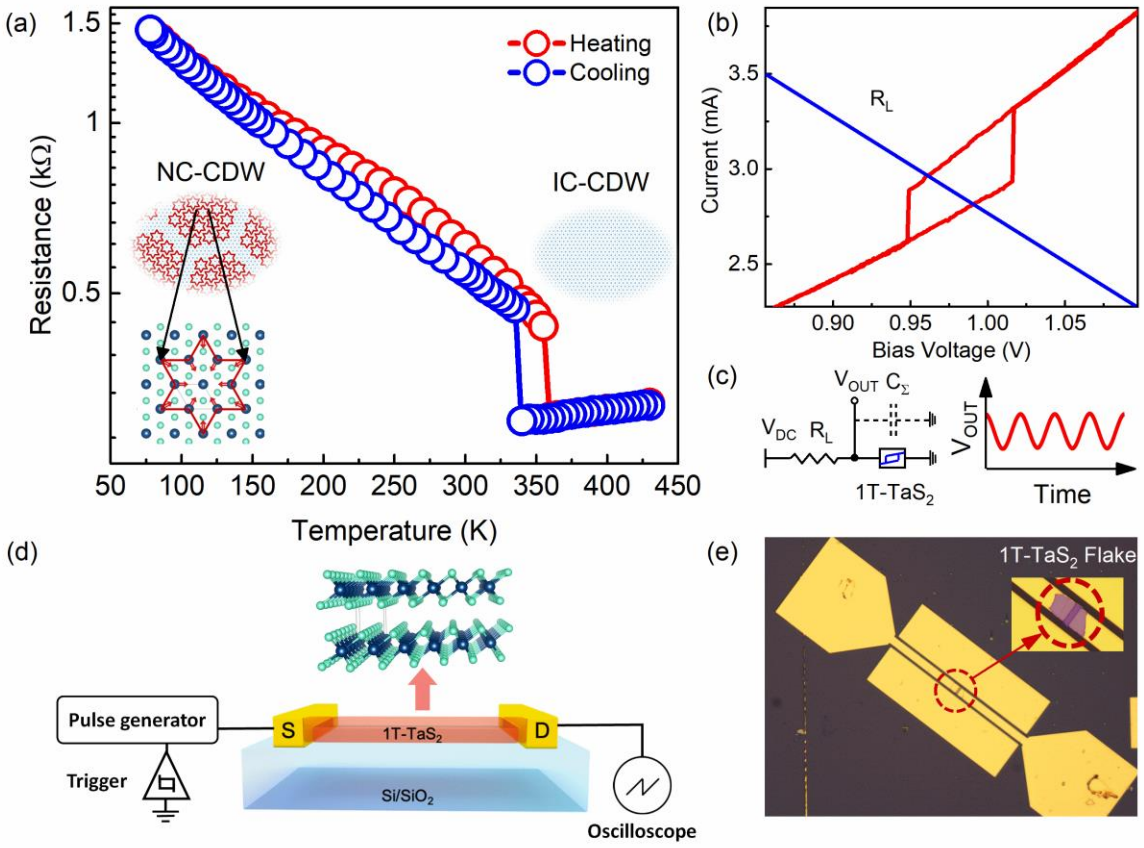

We studied the switching transition between the nearly commensurate and incommensurate CDW phases in 1T-TaS_2 films using pulse measurements and numerical simulations.

A pulse generator creates repetitive current pulses as short as 8 ns. The generated current is then measured by a mixed-signal oscilloscope.

A. Mohammadzadeh, *et al.*, Appl. Phys. Lett. 118, 093102 (2021).

Experimental and Calculated CDW Current-Voltage Characteristics

Experimental

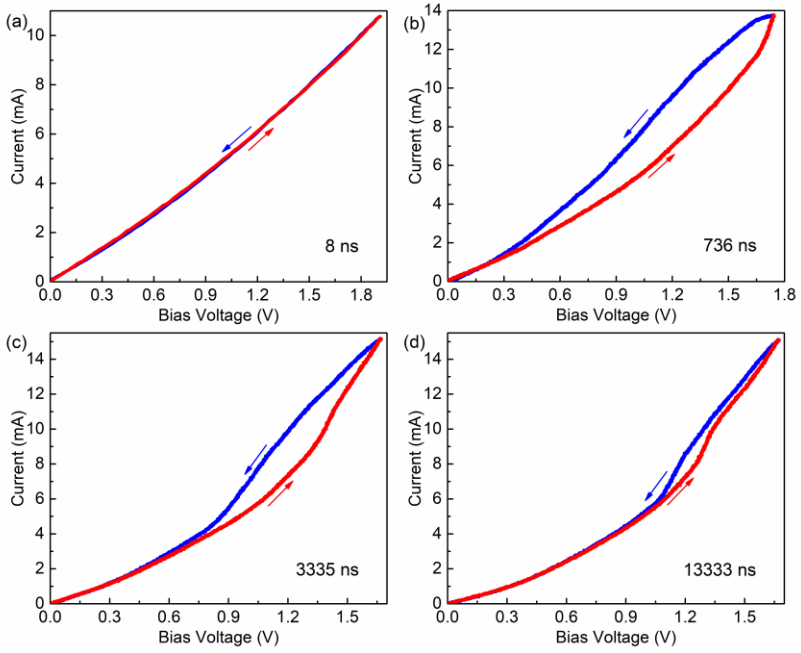

Simulated

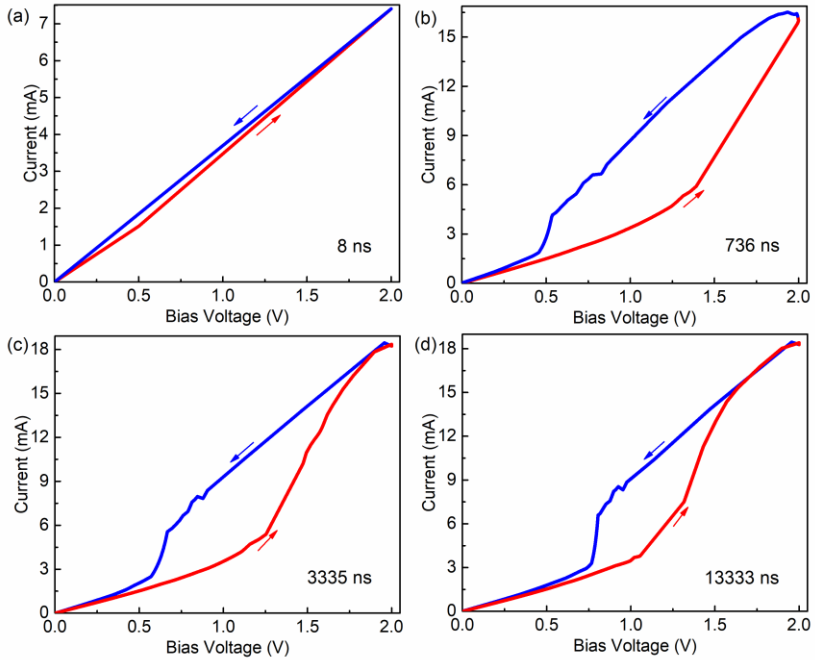

Experimental (left) and simulated (right) I-V characteristics for (a) 8 ns, (b) 736 ns, (c) 3,335 ns, and (d) 13,333 ns pulses. For the shortest duration shown (8 ns), no hysteresis window is observed. With increasing the pulse duration, the width of the hysteresis window expands and then shrinks again. This behavior is attributed to the transient heat diffusion characteristics of the 1T-TaS_2 film, during the up and down sections of the pulse, causing the film to attain different temperatures at fixed bias in the hysteresis region.

A. Mohammadzadeh, *et al.*, Appl. Phys. Lett. 118, 093102 (2021).

Thermally Driven CDW Switching

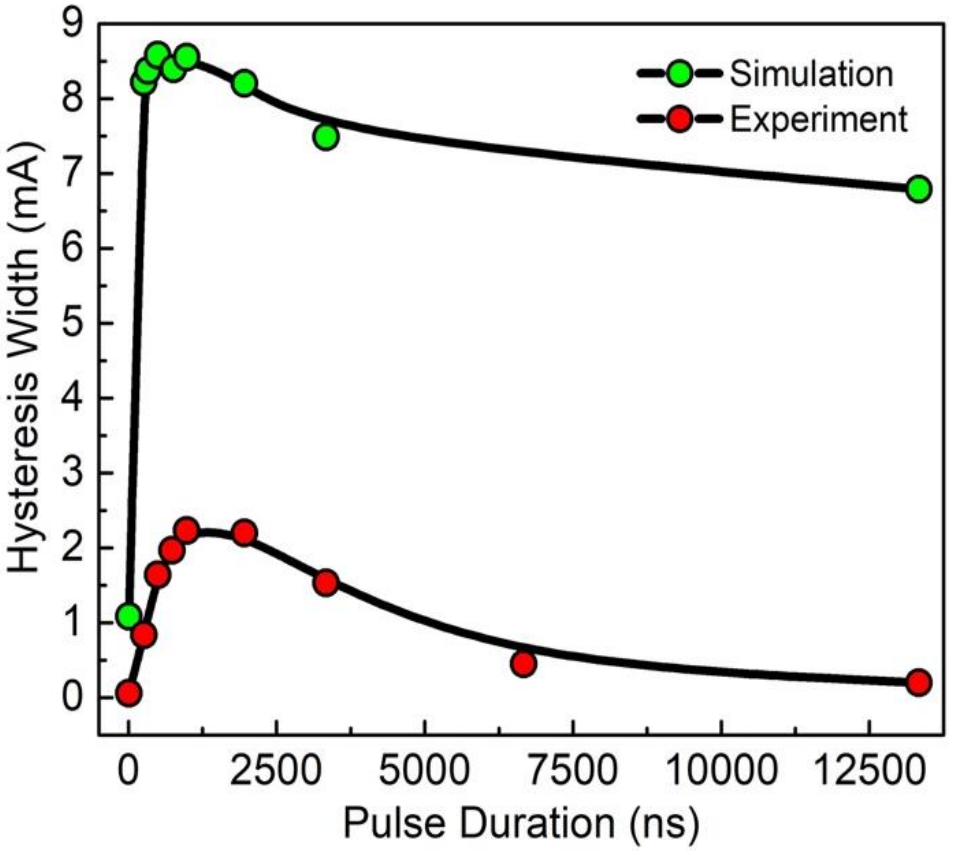

→ Experimental, and simulated hysteresis window width (I_c -I_h) calculated at the constant bias voltage of 1 V as a function of pulse duration. The experimental and theoretical results both follow the same trend, exhibiting a peak at shorter pulse durations and saturating at longer pulse times.

→ Our results do not mean that you cannot achieve electrical switching

A. Mohammadzadeh, S. Baraghani, S. Yin, F. Kargar. J. P. Bird, and A. A. Balandin, "Evidence for a thermally driven charge-density-wave transition in 1T-TaS_2 thin-film devices: Prospects for GHz switching speed" Appl. Phys. Lett., 118, 093102 (2021).

CDW Switching: Prospects of GHz Switching Speed

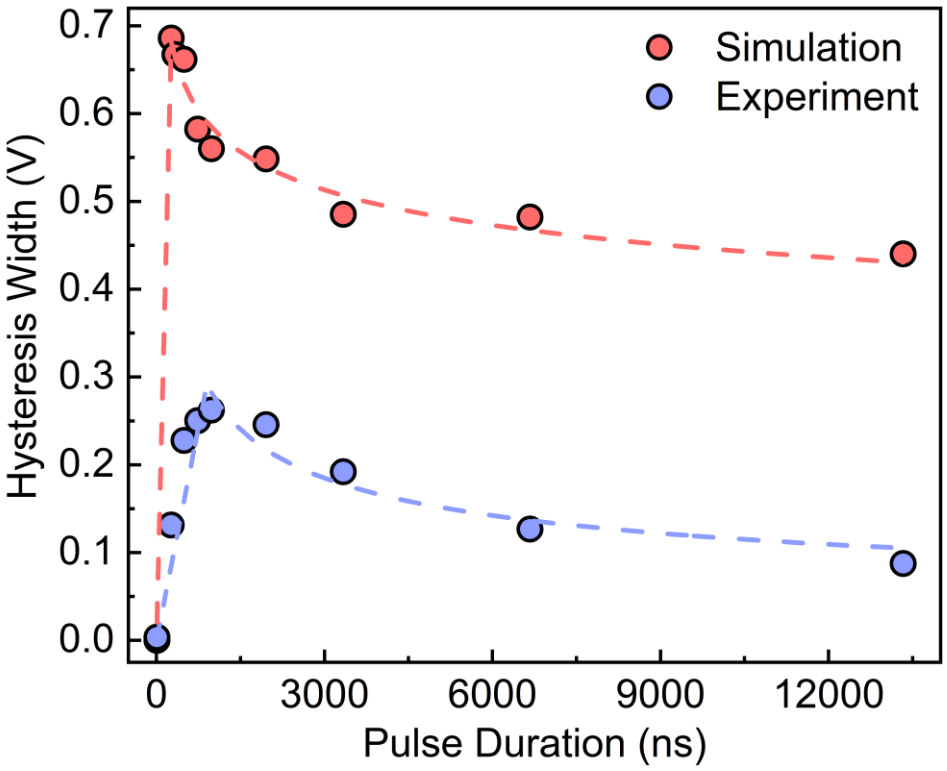

Experimental and simulated hysteresis window width (V_C-V_H) at the constant current of 8 mA and as a function of pulse duration.

We used the experimentally validated model to estimate the device switching speed as the device size decreases. It was found that despite the dominant self-heating effects, tuning of the dimensions can lead to a device that can operate at GHz frequencies.

A. Mohammadzadeh, S. Baraghani, S. Yin, F. Kargar, J. P. Bird, and A.A. Balandin, Thermally-driven charge-density-wave transitions in 1T-TaS_2 thin-film devices: Prospects for GHz switching speed, Appl. Phys. Lett. 118, 093102 (2021) - chosen as the APL Editor's Pick.

Why We Do Not See Depinning and Sliding Clearly in Quasi-2D CDW Materials?

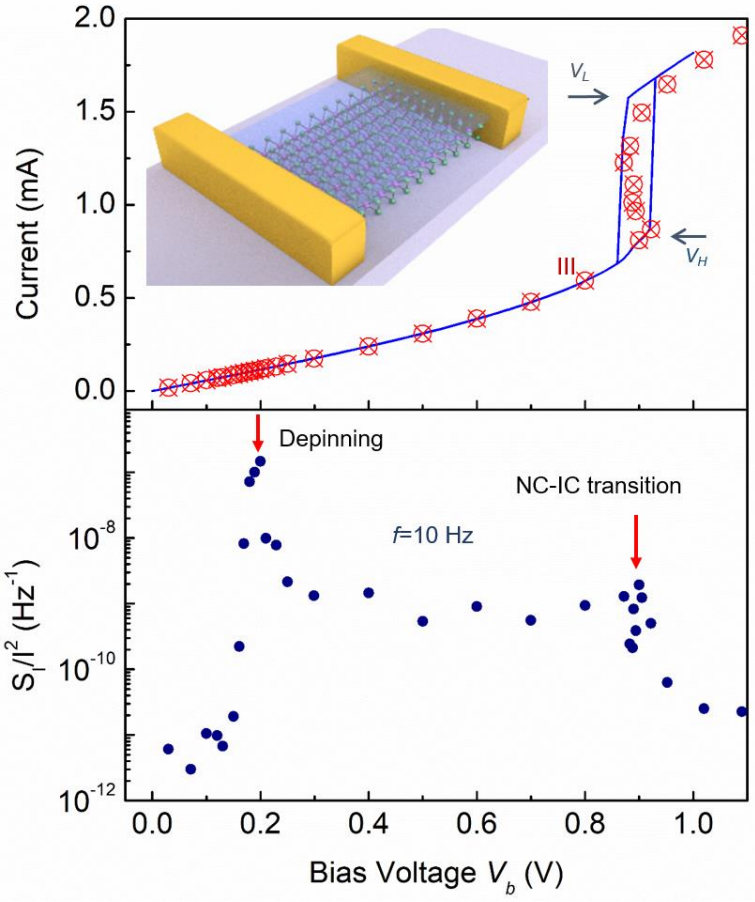

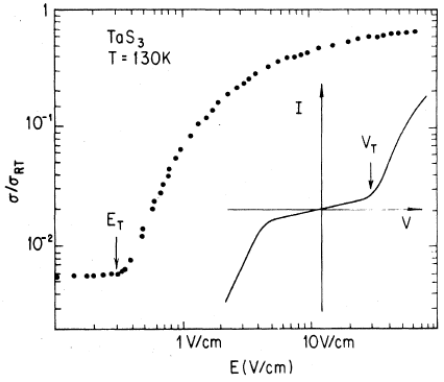

IV-characteristics of 2D CDW materials are different from those of bulk 1D CDW.

G. Gruner, Rev. Mod. Phys., 60, 1129 (1988).

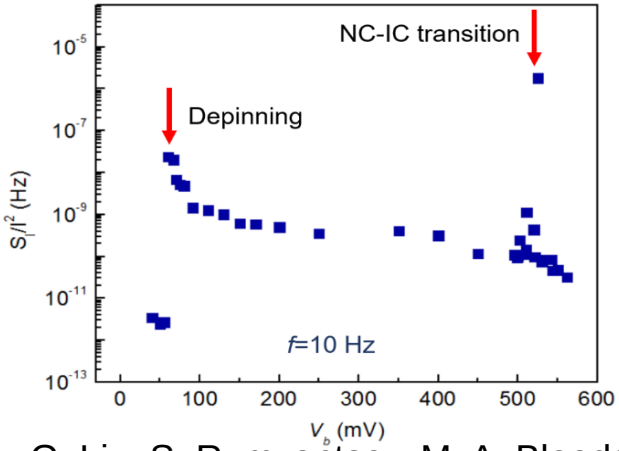

Noise is more sensitive than I-Vs for monitoring CDWs in quasi-2D materials

G. Liu, S. Rumyantsev, M. A. Bloodgood, T. T. Salguero, and A. A. Balandin, Nano Letters, 18, 3630 (2018).

Low-Frequency Noise of the CDW Phase Transitions in 2D Materials

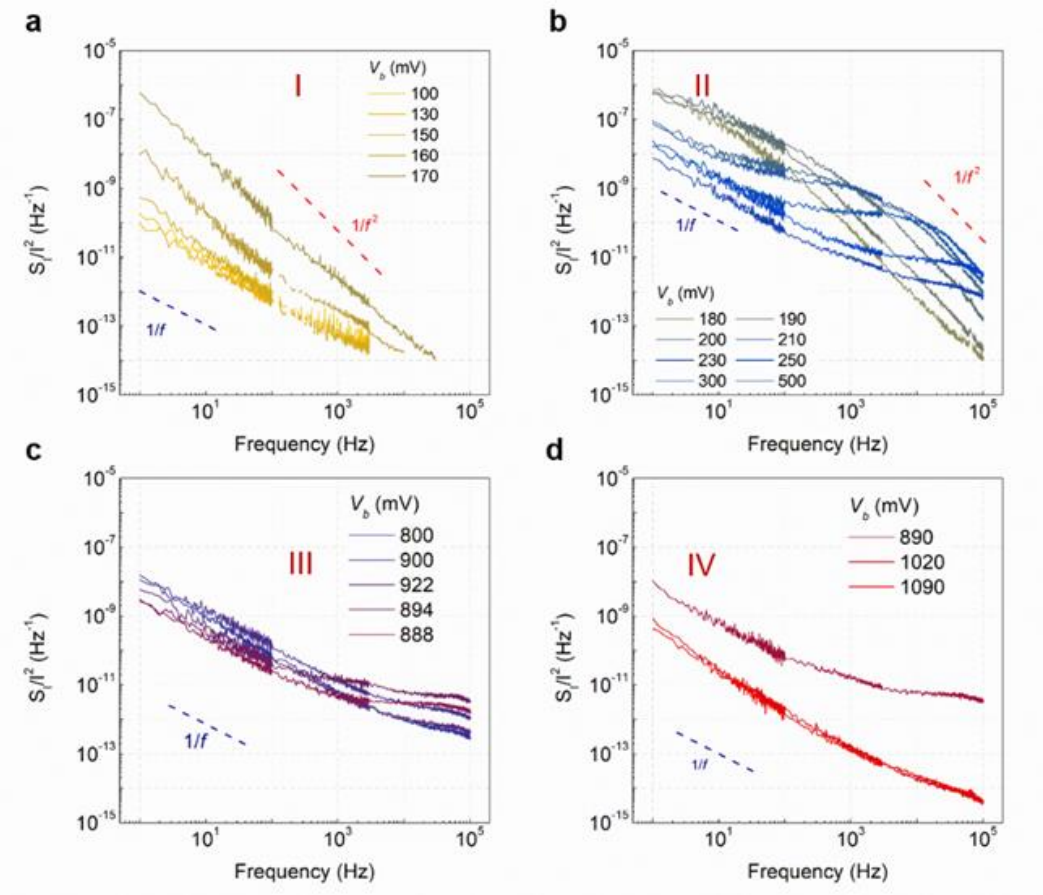

Figure: (a) S_I/I^2 for the bias region I. Below V_b=150 mV, the noise is of 1/f – type. Above 150 mV, the noise spectrum starts to change to $1/f^2$ – type, which is indicative of the Lorentzian "tail". (b) S_I/I^2 for the bias region II. At V_b=180 mV, the noise spectrum evolves into a Lorentzian shape with a corner frequency f_c=10 Hz. As V_b increases, fc shits to 80.5 kHz at 300 mV. Above V_b=300 mV, fc stops moving to higher frequencies. (c) S_I/I^2 for the bias region III. The noise level reaches its maximum at the NC-IC point. (d), S_I/I^2 for the bias region IV. As V_b drives the 1T-TaS_2 into the IC-CDW phase, the noise level reduces and its shape returns to 1/f – type.

Current Fluctuations of the CDWs in the Time Domain

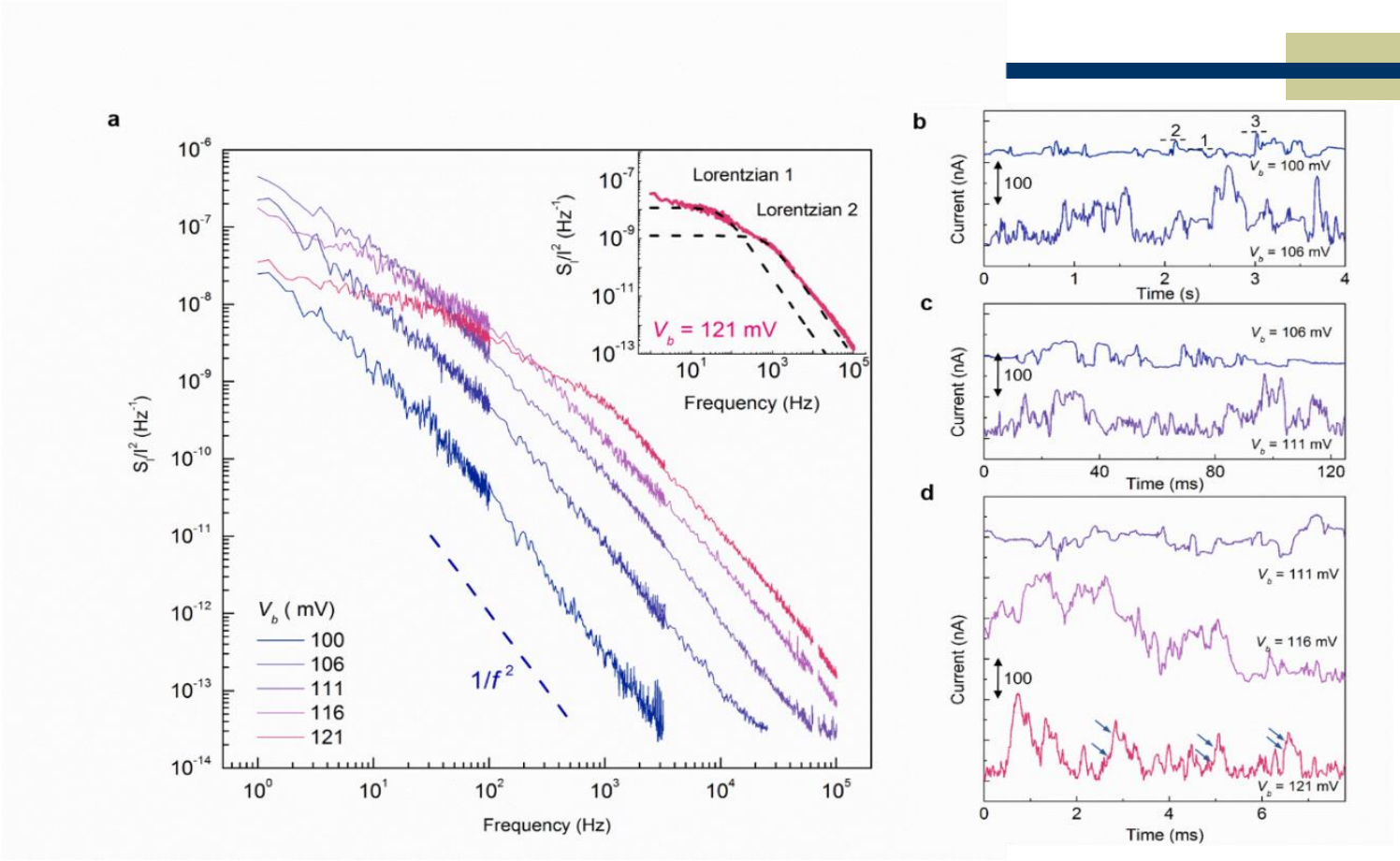

G. Liu, S. Rumyantsev, M. A. Bloodgood, T. T. Salguero, and A. A. Balandin, Nano Letters, 18, 3630 (2018).

Current Oscillations in Bulk Quasi-1D CDW Materials

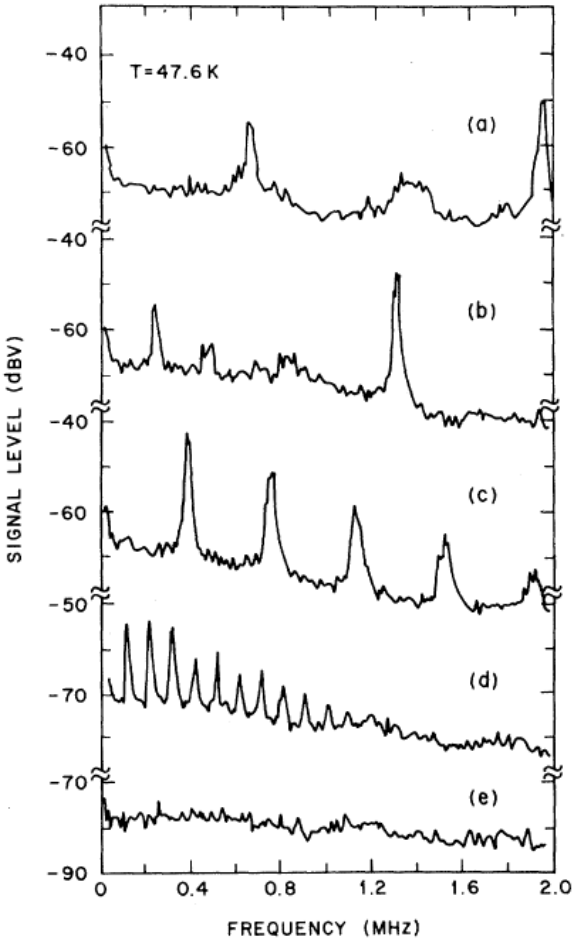

Sliding-Mode Conductivity in $NbSe_3$: Observation of a Threshold Electric Field and Conduction Noise

R. M. Fleming and C. C. Grimes
Bell Laboratories, Murray Hill, New Jersey 07974
(Received 15 March 1979)

FIG. 3. Output of on-line spectrum analyzer for selected values of current. Increasing current from zero (e) to a value above threshold (d) results in an increase of broad-band noise plus a discrete frequency with numerous harmonics. The frequency increases with current and at higher currents (b) a second frequency appears. Currents and dc voltages (a) $I = 270\ \mu A$, $V = 5.81$ mV, (b) $I = 219\ \mu A$, $V = 5.05$ mV, (c) $I = 154\ \mu A$, $V = 4.07$ mV, (d) $I = 123\ \mu A$, $V = 3.40$ mV, (e) $I = V = 0$. Sample cross section $\approx 136\ \mu m^2$.

"Narrow band noise" was considered to be a direct evidence of CDW de-pinning and sliding.

The Signatures of the “Narrow Band Noise” in Quasi-2D CDWs

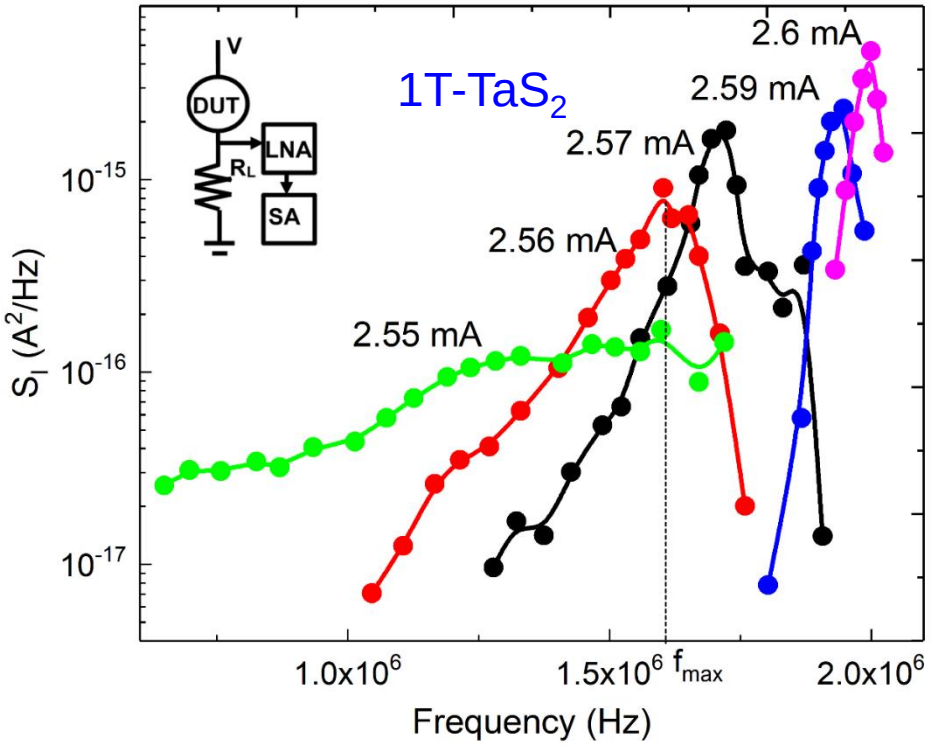

Noise as a function of frequency for several value of the current through the device channel. The peak shifts to the higher frequency f_o with the increasing current.

In bulk quasi-1D CDW materials, the linear relationship was explained assuming that f is proportional to the CDW drift velocity, v_D, so that $f=v_D/\Lambda$, where Λ is the characteristic distance.

Since $I_{CDW}=nef\Lambda A$, where n is the charge carrier density, e is the charge of an electron, and A is the cross-sectional area, one obtains: $f=(1/neLA)\times I_{CDW}$

A. K. Geremew, S. Rumyantsev, B. Debnath, R. K. Lake, and A. A. Balandin, "High-frequency current oscillations in charge-density-wave 1T-TaS2 devices: Revisiting the “narrow band noise” concept," Appl. Phys. Lett., 116, p. 163101 (2020).

Have We Found the "Narrow Band Noise" in Quasi-2D CDWs?

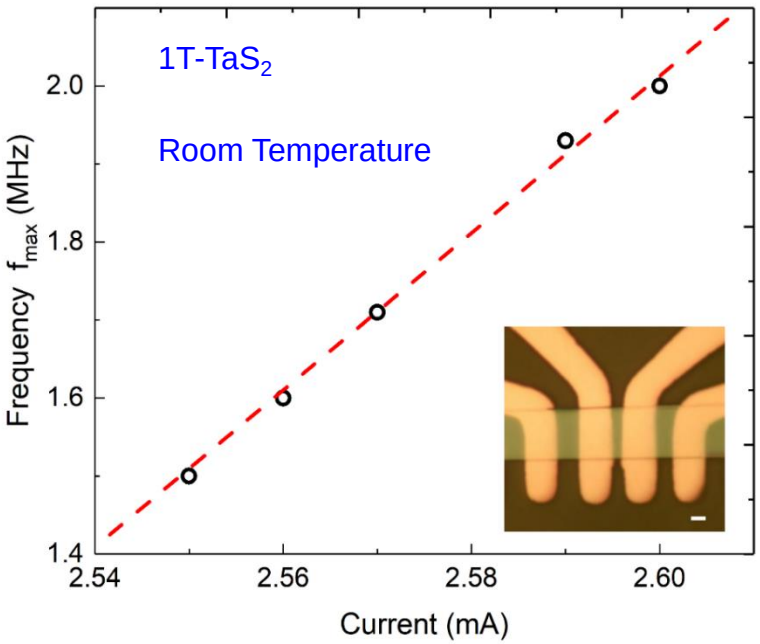

Frequency, f_0 of the noise peaks as a function of the current through 1T-TaS_2 device channel. The inset shows a microscopy image of a representative 1T-TaS_2 device structure with several metal contacts.

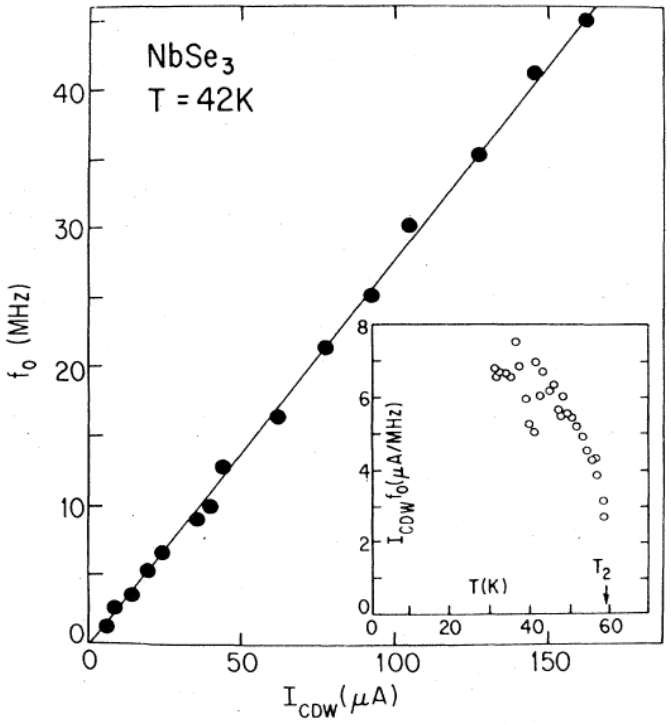

Relation between the COW current and fundamental oscillation frequency in $NbSe_3$. The inset shows I_{CDW}/f_0 vs. temperature. After Bardeen et al. (1982).

The Current Oscillations are due to Hysteresis at the NC-CDW – IC-CDW Transition

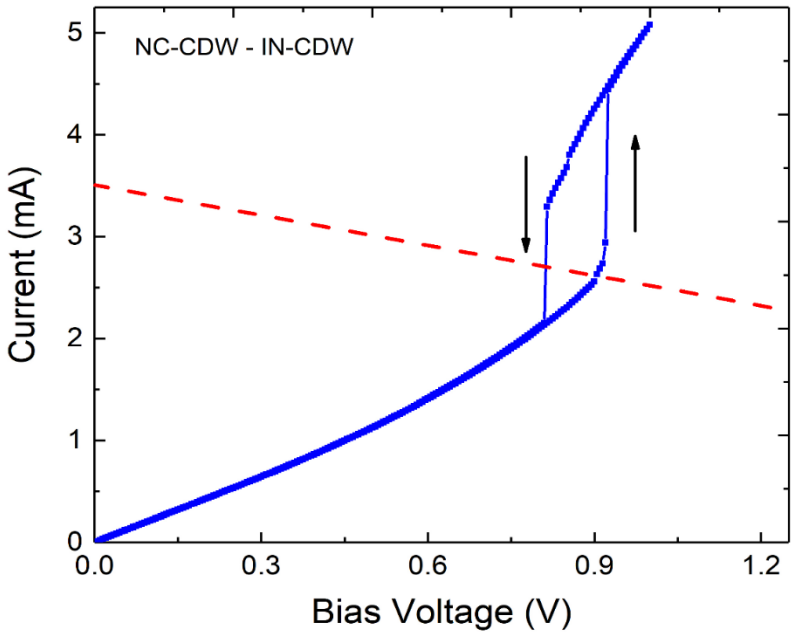

I-Vs of tested 1T-TaS_2 device which revealed "narrow band noise". The hysteresis loop at the bias voltage V = 0.9 V corresponds to the transition from the NC-CDW phase to the IC-CDW phase induced the applied electric field.

The current oscillations appear to be similar to our earlier result – this is not the "narrow band noise."

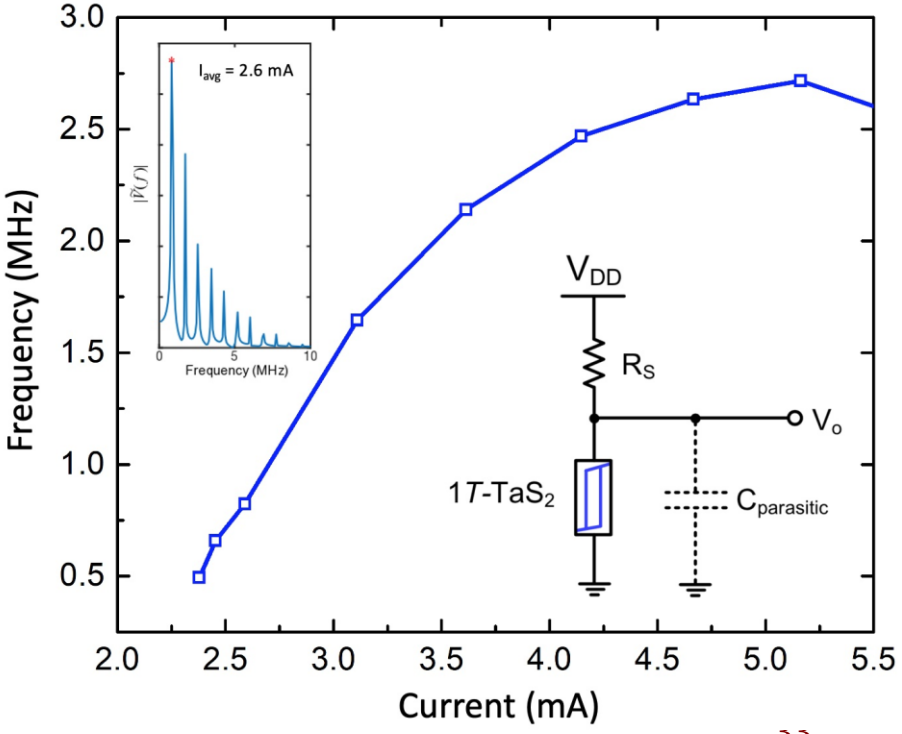

Closer Look at I-Vs of 2D CDW Devices

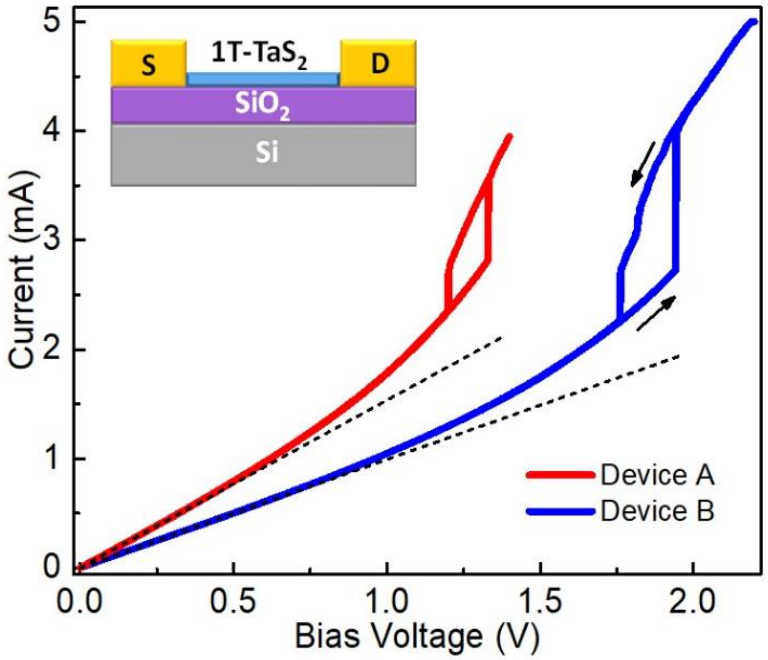

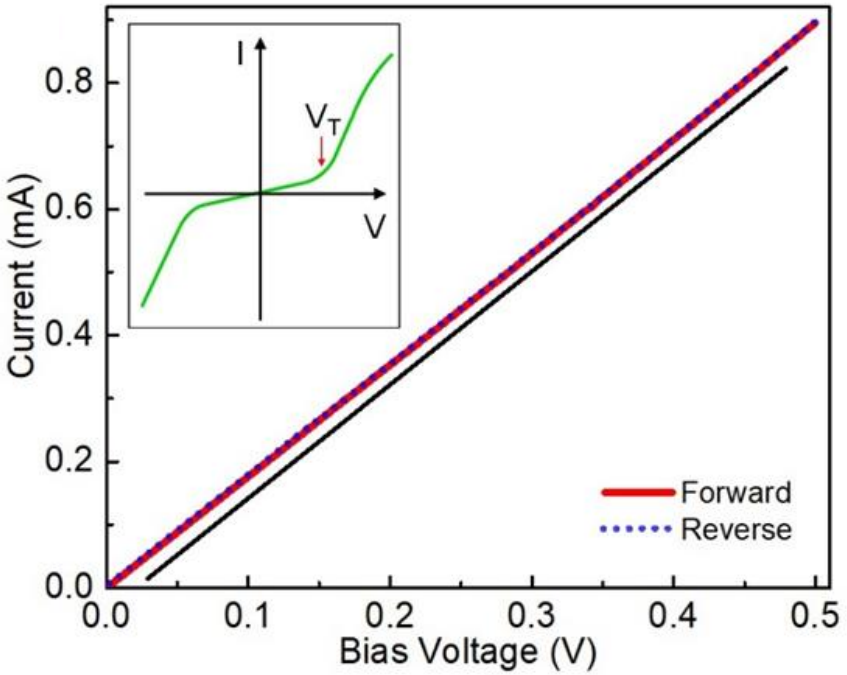

Current-voltage characteristic of the 1T-TaS_2 devices on Si/SiO_2 substrate at room temperature. The direction of the current sweep is indicated with the arrows. The data are presented for two devices with different channel length fabricated on the same structure. The arrows indicate the direction of the current sweep.

Derivatives of the I-V Characteristics

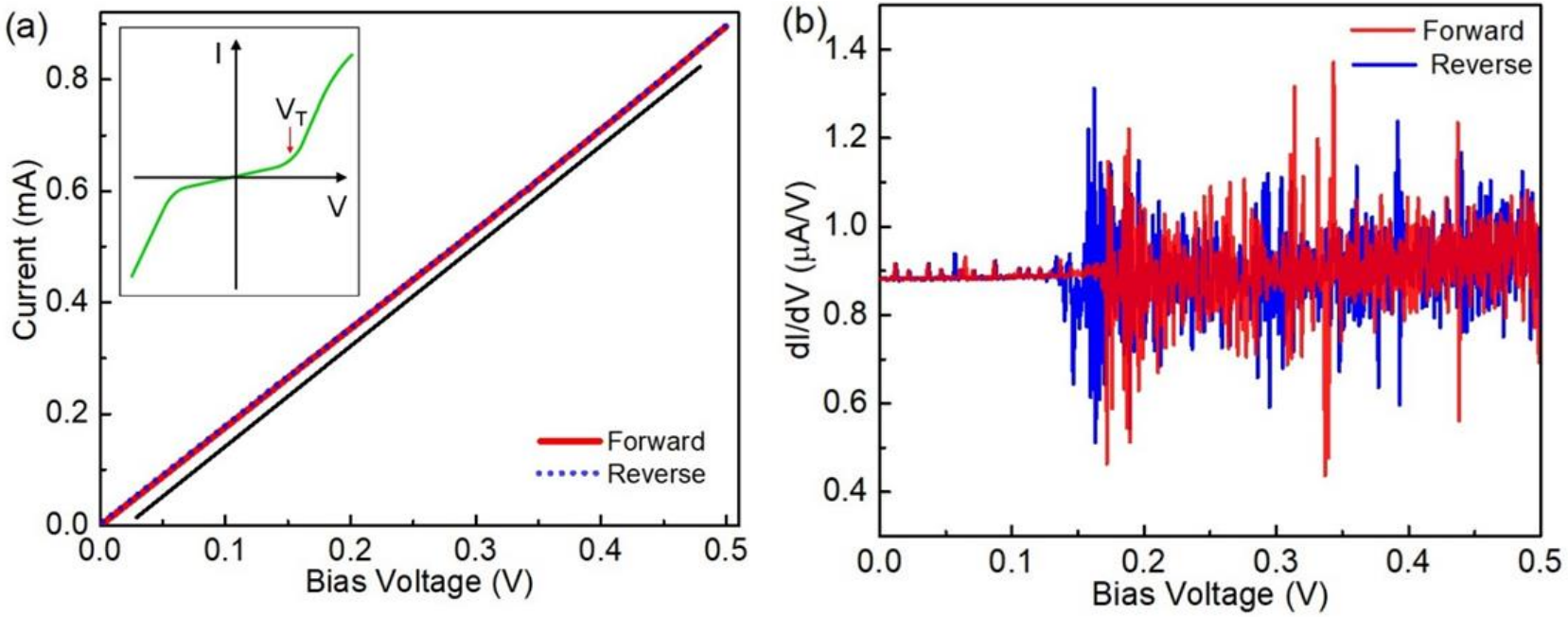

(a) The current in the forward (red) and reverse (blue) sweeping overlaps. The straight black line is shown for comparison. No deviations from the non-linearity are observed in this bias range. (b) The derivative of current-voltage characteristics revealing a strong change in the electron transport.

The threshold in 2D is ~1 kV/cm while in 1D systems it is ~ 40 mV/cm – 4 V/cm

Noise Spectroscopy Reveals the Depinning in 2D 1T-TaS_2 CDW Devices

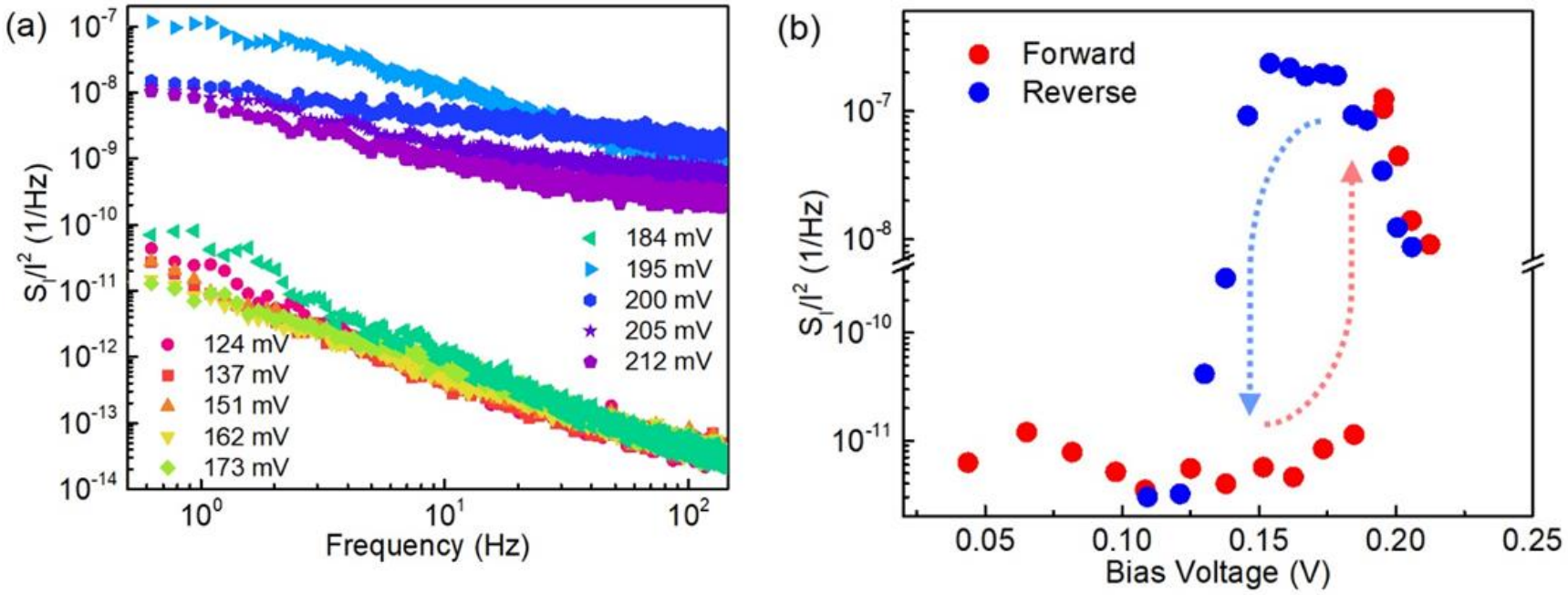

A. Mohammadzadeh, A. Rehman, F. Kargar, S. Rumyantsev, J. M. Smulko, W. Knap, R. K. Lake, and A. A. Balandin, "Room-temperature depinning of the charge-density waves in quasi-2D 1T-TaS2 devices", Appl. Phys. Lett., 118, 223101 (2021).

Likely Signatures of Sliding CDWs in 2D Materials

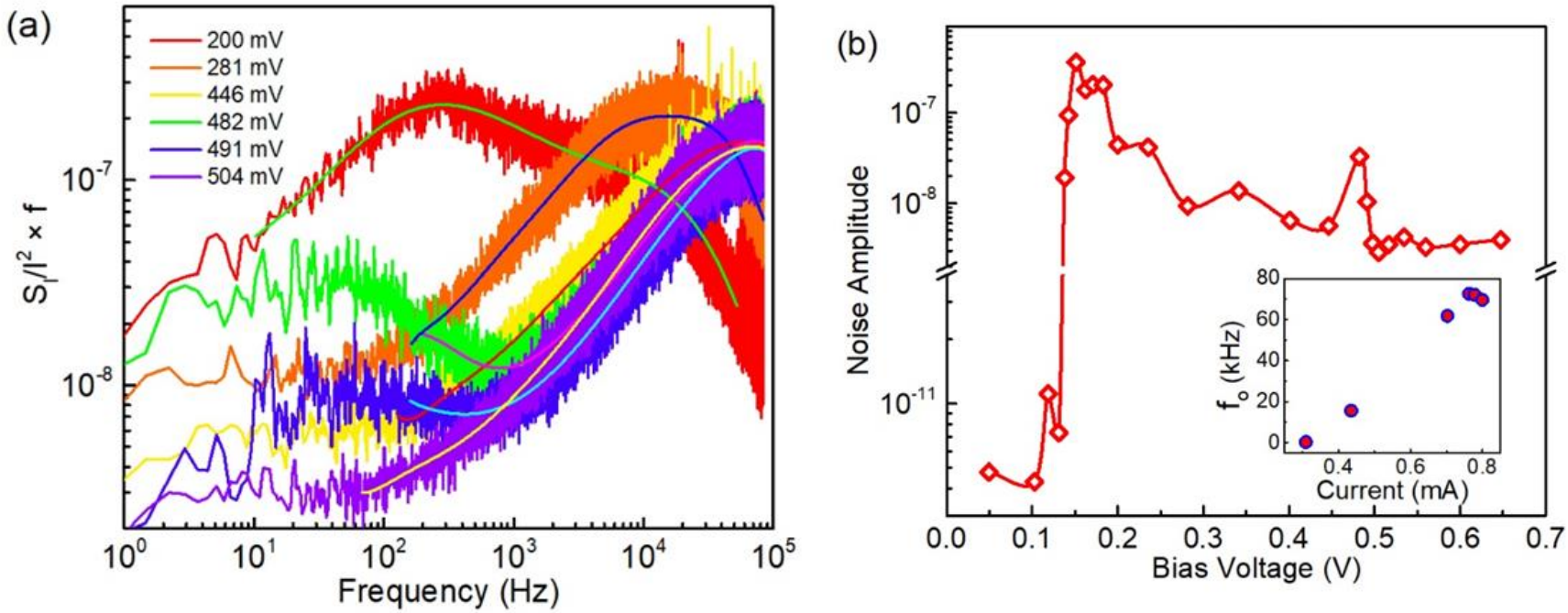

(a) Normalized noise spectral density multiplied by the frequency, $S_I/I^2 \times f$, as a function of frequency at different applied bias voltages. (b) The noise amplitude as a function of the bias voltage. Note the break in the y-axis. The noise level experiences a drastic increase at the depinning point. The inset shows the dependence of the corner frequencies with the current in the device channel.

→ Extremely small contribution of CDW current to the total current in 2D systems

Part – IV: 1D Van der Waals Materials

Can we exfoliate Quasi-1D atomic threads like we do quasi-2D atomic planes?

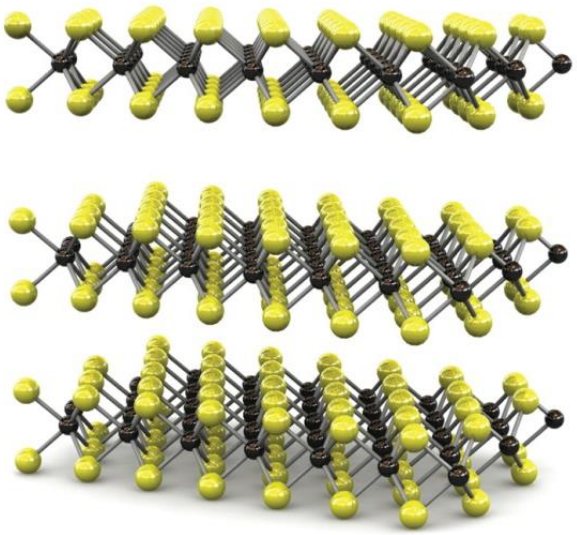

MoS_2

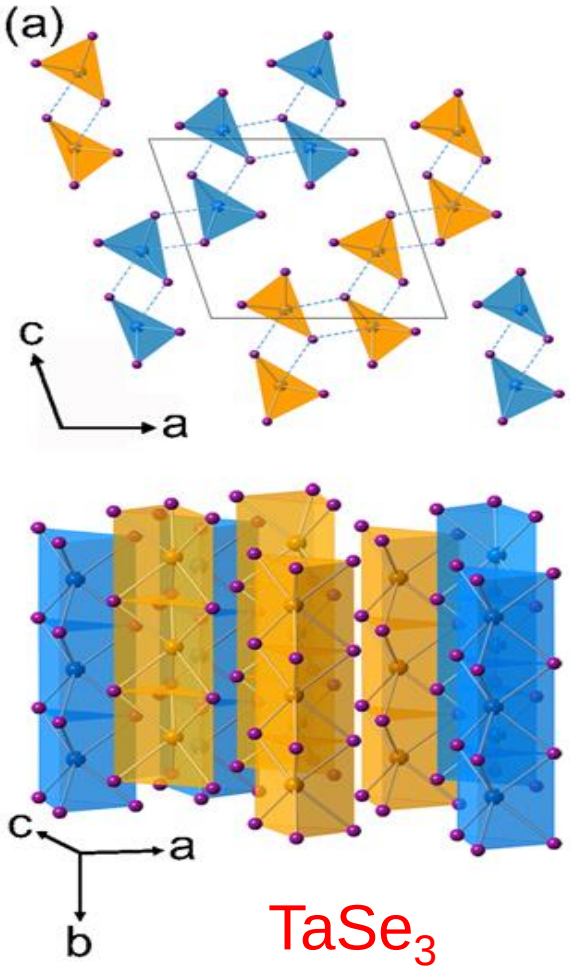

$TaSe_3$

→ Crystal structure of monoclinic $TaSe_3$, with alternating layers of $TaSe_3$

→ Cross section of the unit cell, perpendicular to the chain axis (b axis).

→ The side view: 1D nature of $TaSe_3$ chains along the b axis.

Boron Nitride Capped Devices with Quasi-1D $TaSe_3$ Channels

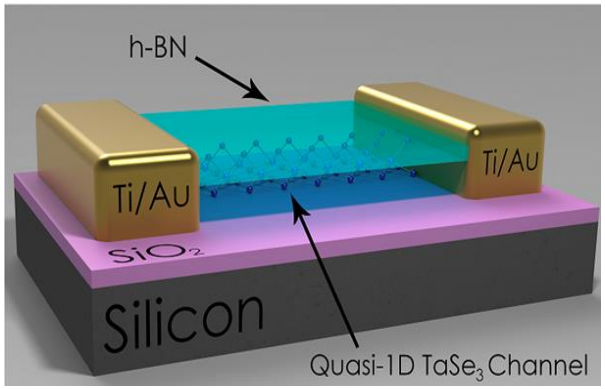

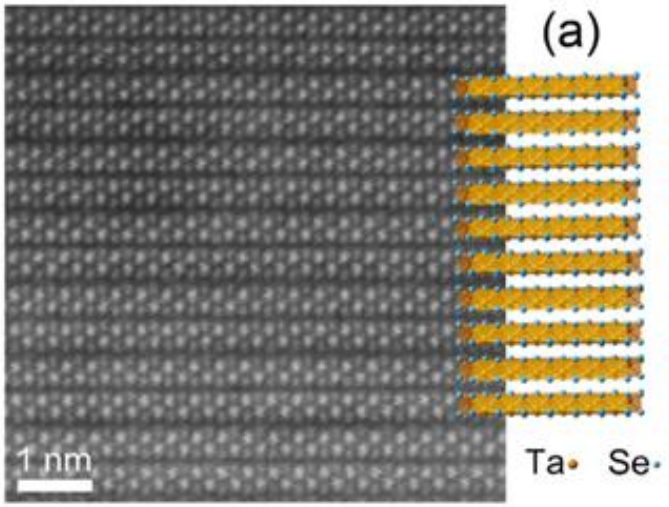

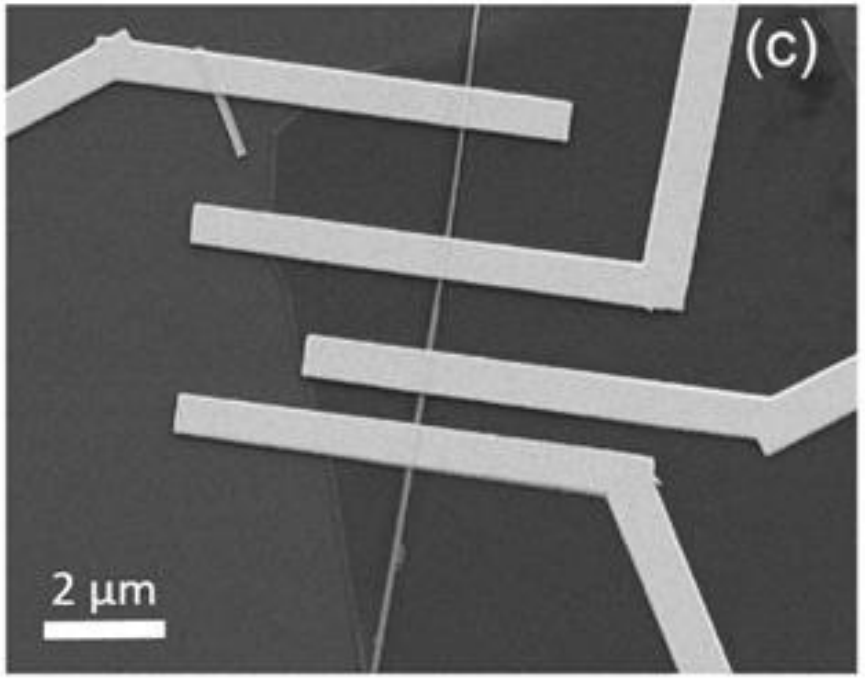

M.A. Stolyarov, G. Liu, M.A. Bloodgood, E. Aytan, C. Jiang, R. Samnakay, T.T. Salguero, D.L. Nika, S.L. Rumyantsev, M.S. Shur, K.N. Bozhilove and A.A. Balandin, Breakdown current density in h-BN-capped quasi-1D $TaSe_3$ metallic nanowires, *Nanoscale*, **8**, 15774 (2016)

Low-Field Electrical Characteristics of Devices with Quasi-1D $TaSe_3$ Channels

- Current-voltage characteristics of $TaSe_3$ devices with different channel length.
- Linear characteristics at low voltage indicates good Ohmic contact of $TaSe_3$ channel with the metal electrodes.

The contact resistance extracted from TLM data is $2R_C$=22 Ω-μm

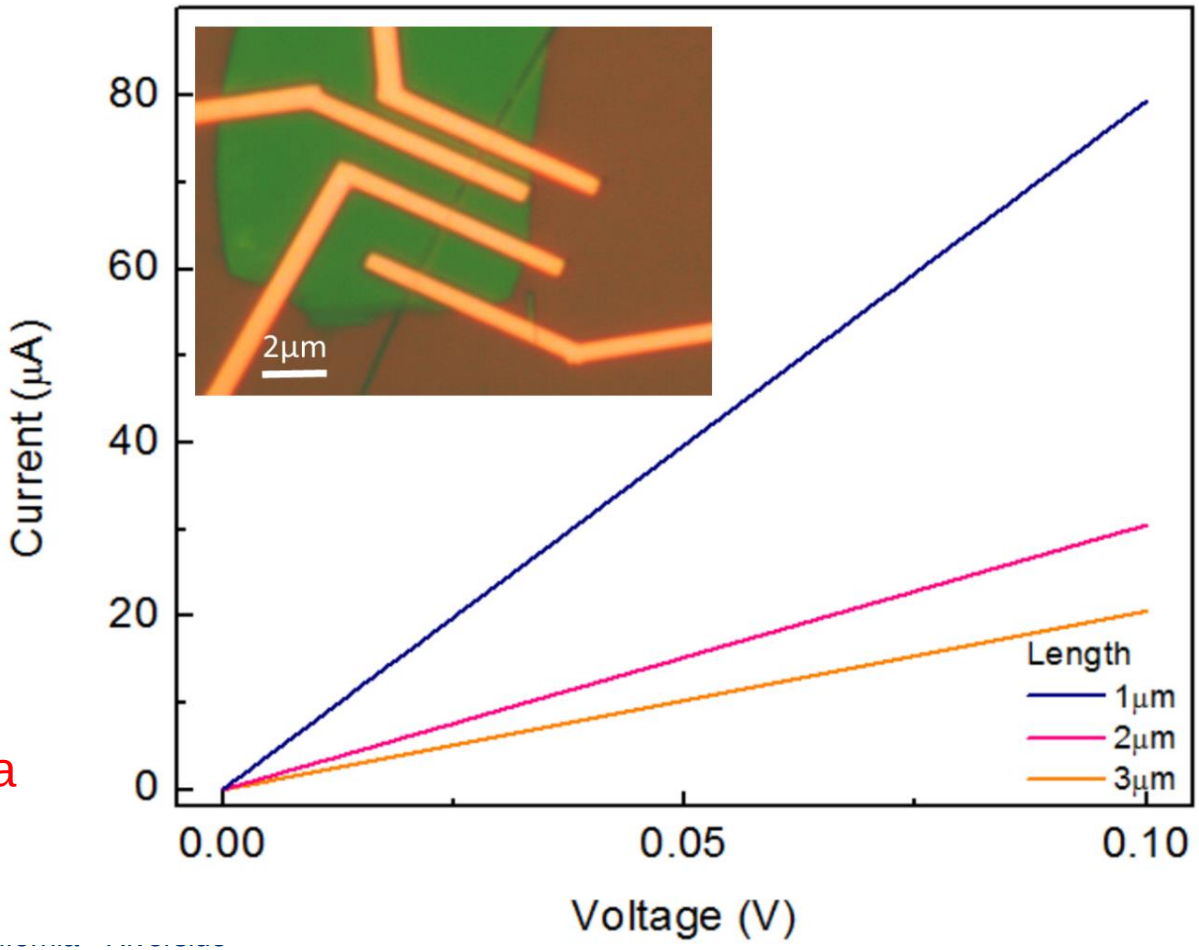

Current Density in Quasi-1D $TaSe_3$ Nanowires

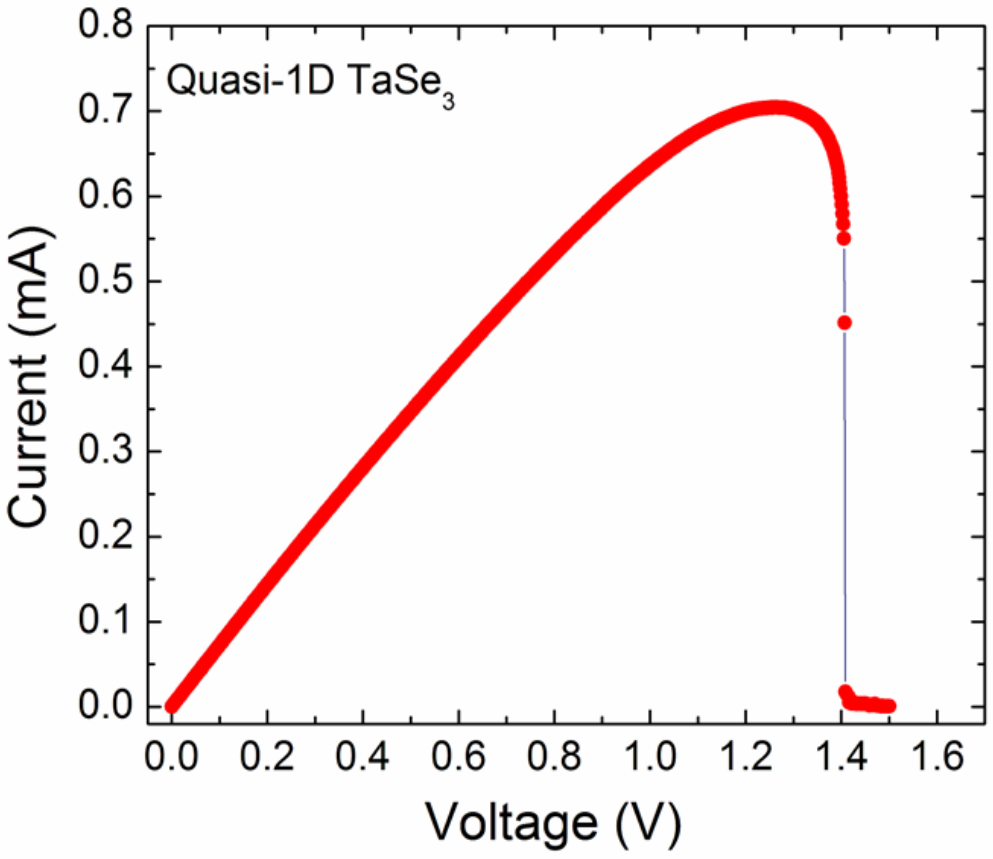

Resistivity is 2.6 – 6.4×10^{-4} Ω-cm.

→ High-field I-V characteristics showing the breakdown point. In this specific device the breakdown is gradual.

→ Breakdown current density of about 32 MA/cm^2 — an order-of-magnitude higher than that for copper.

M.A. Stolyarov, G. Liu, M.A. Bloodgood, E. Aytan, C. Jiang, R. Samnakay, T.T. Salguero, D.L. Nika, S.L. Rumyantsev, M.S. Shur, K.N. Bozhilove and A.A. Balandin, Breakdown current density in h-BN-capped quasi-1D $TaSe_3$ metallic nanowires, *Nanoscale*, **8**, 15774 (2016)

Extracting Electromigration Information from Temperature Dependent Noise Data

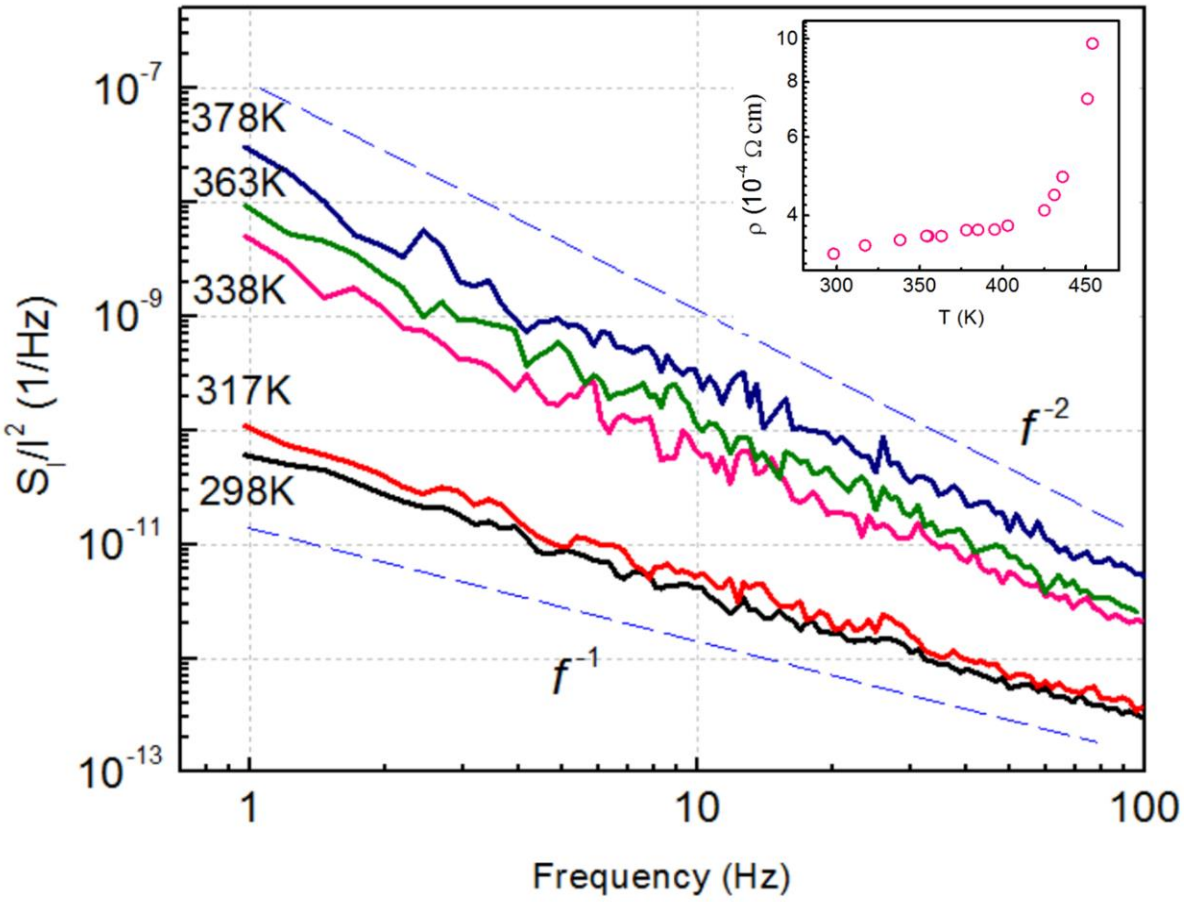

The 1/f noise at RT becomes more of $1/f^2$ – type at elevated temperatures. The increased frequency power factor γ suggests the onset of the electromigration processes.

Inset shows the temperature dependent resistance of the quasi-1D $TaSe_3$ nanowire.

The graduate increase of the resistance with temperature, for T < 410 K is typical for metal. The sharply rising resistance for T > 410 K indicates the occurrence of electromigration.

Noise Analysis: Dutta–Horn Model

Correlation of the frequency power factor γ with the noise (electromigration) activation energy E_P

$$\gamma(T) = 1 - \frac{1}{\ln(2\pi f \tau_0)}\left(\frac{\partial \ln S(f,T)}{\partial \ln T} - 1\right)$$

$$S(f,T) \propto \frac{kT}{2\pi f} D(E)$$

$$E_P = -kT\, ln(2\pi f \tau_0)$$

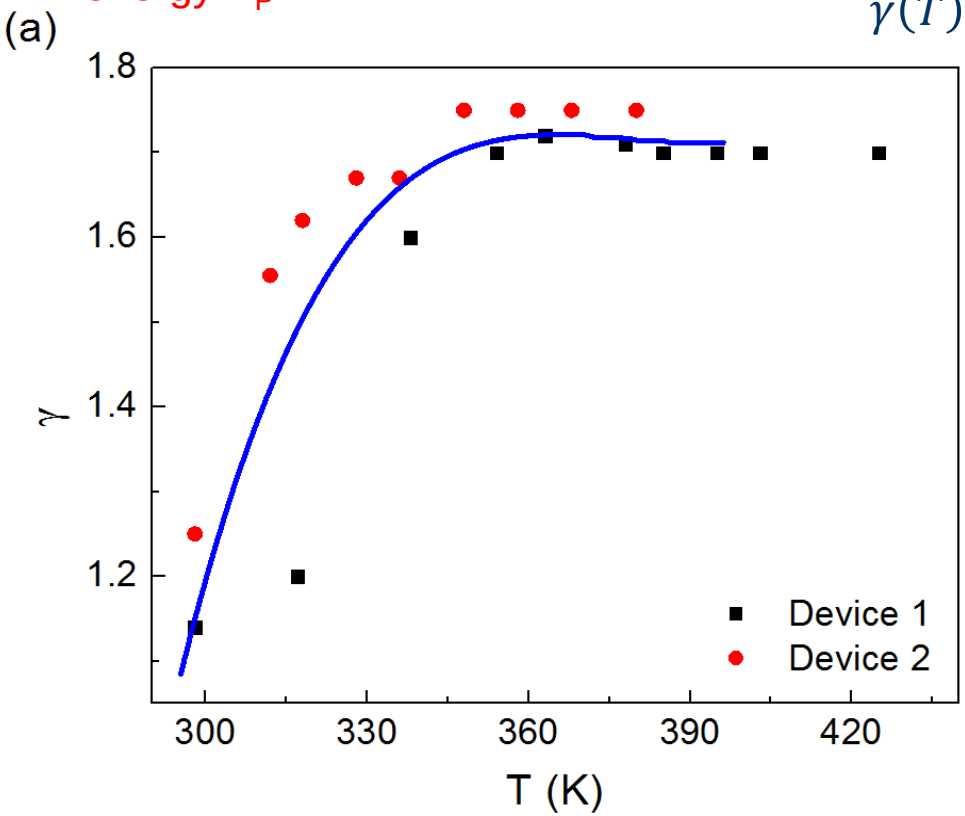

G. Liu, S. Rumyantsev, M. A. Bloodgood, T. T. Salguero, M. Shur, and A. A. Balandin, "Low-frequency electronic noise in quasi-1D $TaSe_3$ van der Waals nanowires," Nano Lett., 17, 377 (2017).

Noise Spectroscopy of the $ZrTe_3$ Quasi-1D van der Waals Nanoribbon Devices

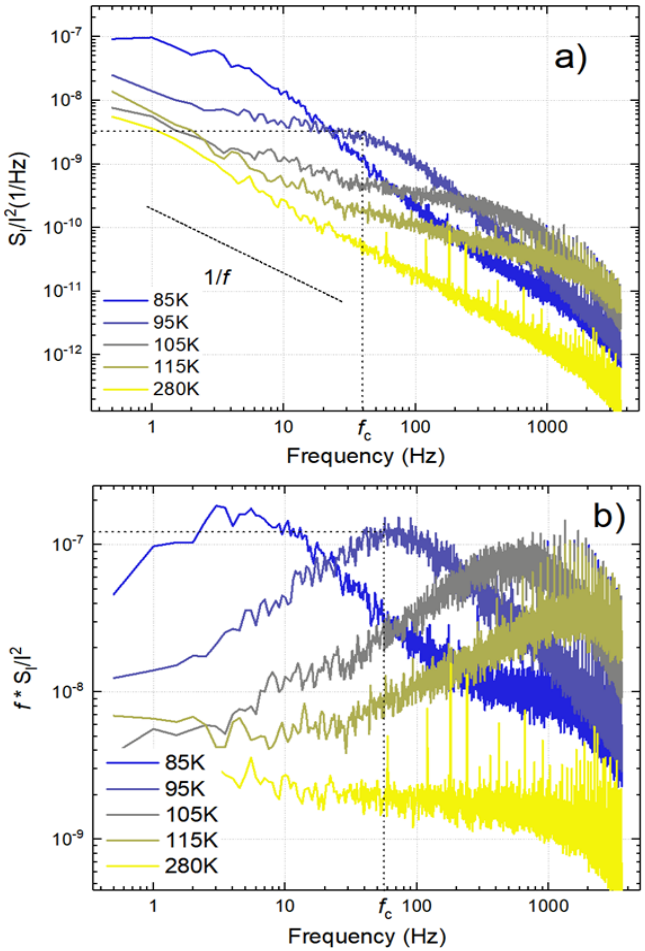

(a) Normalized noise spectral density, S_I/I^2, as a function of frequency of quasi-1D $ZrTe_3$ nanoribbon at temperatures from 85 K to 280 K.

(b) Normalized noise spectral density multiplied by frequency, $S_I/I^2 \times f$, as a function of frequency. Note an unusually strong dependence of the Lorentzian peak on the temperature (at bias 0.1 V)The position of characteristics frequency, *f*c, is shown in broken line.

$$\frac{S_I}{I^2} = \frac{4N_t}{Vn^2}\frac{\tau F(1-F)}{1+(\omega\tau)^2} \qquad \frac{1}{\tau} = \frac{1}{\tau_c} + \frac{1}{\tau_e}$$

$$\tau_c = \frac{1}{\sigma v_T n} \qquad \tau_e = \frac{1}{\sigma v_T N_c \exp\left(-\frac{E_0}{kT}\right)}$$

Trap Activation Energies in $ZrTe_3$ Quasi-1D van der Waals Nanoribbon Devices

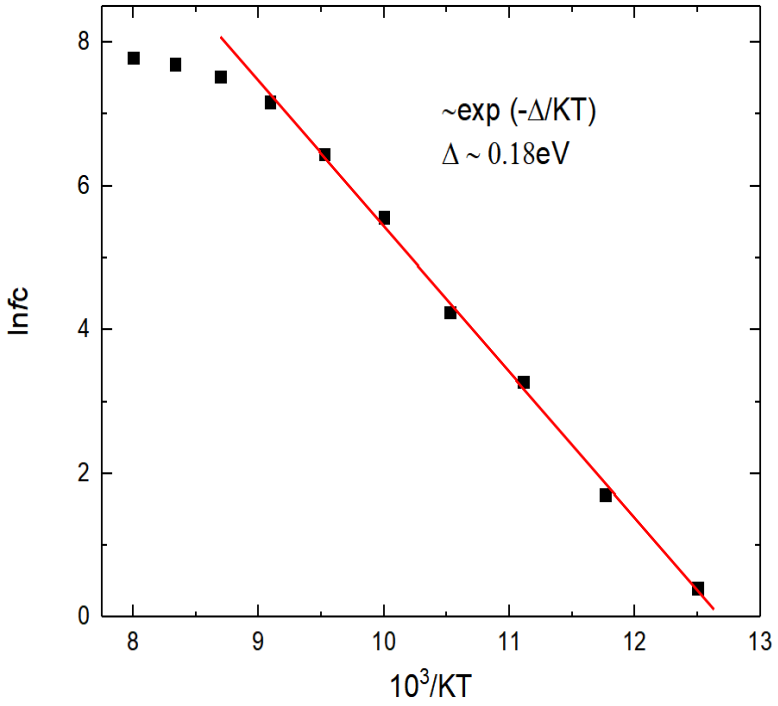

A. K. Geremew, S. Rumyantsev, M. A. Bloodgood, T. T. Salguero, and A. A. Balandin, "Unique features of the generation–recombination noise in quasi-one-dimensional van der Waals nanoribbons," Nanoscale, 10, 19749 (2018).

Arrhenius plot of the characteristics frequency, $\ln(f_c)$, as a function of the inverse of temperature, K^{-1} in quasi-1D $ZrTe_3$ device. This plot was used to extract the activation energy.

The extracted trap activation energy is $E_0 \cong$ 0.18 eV.

$$\sigma = \sigma_0 \exp(-\frac{E_1}{kT}).$$

The activation energy of the cross-section temperature dependence and level position can be easily extracted as E_1=0.144 eV and E_0=0.0456 eV. These data indicate that the activation energy of the characteristic frequencies of the G-R noise peaks is dominated by the activation energy of the capture cross-section.

The Poole-Frenkel Effect or NOT?

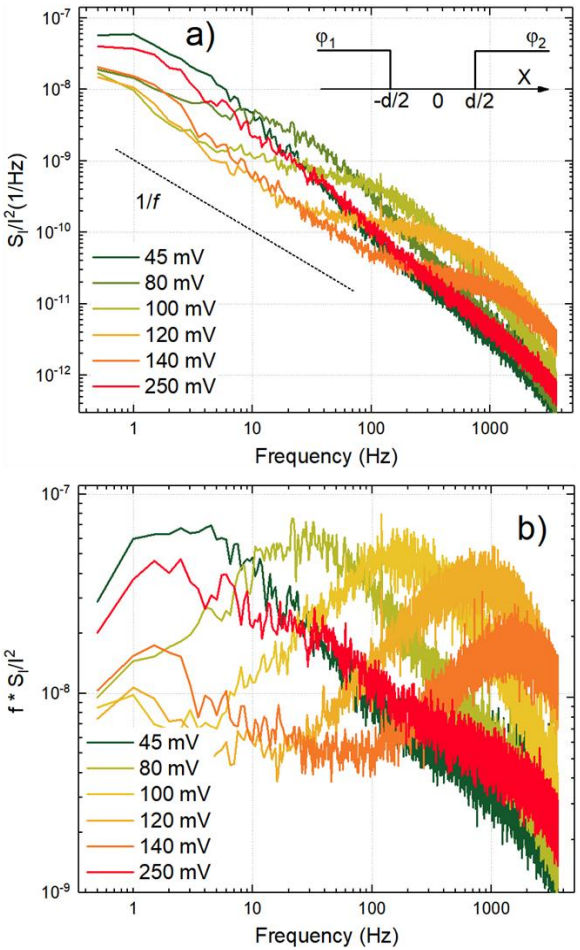

(a) Normalized noise spectral density, S_I/I^2, as a function of frequency of quasi-1D $ZrTe_3$ nanoribbon at the source – drain voltage ranging from 45 mV to 250 mV. Inset shows a schematics of potential barrier height between two states. (b) Normalized noise spectral density multiplied by frequency, $S_I/I^2 \times f$, as a function of frequency. Note an unusually strong dependence of the Lorentzian peak on the source – drain bias (at T =78K).

The shifting of the Lorentzian peak in the noise spectrum with the applied electric field can be due to reducing the impurity barrier potential in high electric field:

$$\Delta E_{fp} = \left(\frac{q^3 F}{\pi \varepsilon_0 \varepsilon}\right).$$

We estimated that the electric filed required to shift this frequency three orders of magnitude is of the order 50 kV/cm. However, for the 2-mm length nanoribbon the average field in the sample does not exceed ~1.25 kV/cm.

$$F\left(\frac{\varphi_1}{x + d/2} - \frac{\varphi_2}{-x + d/2}\right)\frac{1}{\ln L/a}$$

L.D. Landau & E.M. Lifshitz Electrodynamics of Continuous Media (1960)

Conclusions

→ Voltage controlled NC-CDW to IC-CDW transition in two-dimensional 1T-TaS_2 channels can be utilized for switching at RT

→ Low-frequency noise spectroscopy is a powerful tool to investigate electronic transport phenomena in CDW material systems

→ Noise spectroscopy helps to prove radiation hardness of CDW materials

→ The process of depinning and sliding are different in 2D from those in 1D

→ Not all Lorentzians are G-R noise signatures

→ Noise spectroscopy can help to determine activation energies for the electromigration

Acknowledgements